BULGARIAN ACADEMY OF SCIENCES

INSTITUTE OF POLYMERS

INA BORISLAVOVA ANASTASOVA

ELECTROSPUN HYBRID MATERIALS BASED ON POLY(L-LACTIDE-*co*-D,L-LACTIDE) AND CHITOSAN DERIVATIVES WITH PURPOSELY TAILORED DESIGN FOR POTENTIAL BIOMEDICAL APPLICATIONS AND PHOTOCATALYTIC WATER PURIFICATION

DISSERTATION ABSTRACT

presented for acquisition of

the Educational and scientific degree "Doctor"

Professional field: 4.2. Chemical Sciences

Specialty: Polymers and Polymer materials

Scientific supervisors:

Prof. Dr. Olya Stoilova

Prof. Dr. Milena Ignatova

Sofia, 2025

The dissertation was discussed and admitted for defense at a meeting of the Colloquium of the Institute of Polymers – BAS.

The dissertation is presented on 123 pages and includes 35 figures and 2 schemes. 323 references are used. The results are reported in 2 publications and 15 science forums.

The defense of the dissertation will take place on ..…….. 2026 at …….. h in the meeting room of the Institute of Polymers – BAS at a meeting of the scientific jury.

The defense materials are available to the interested ones in the office of the Institute of Polymers – BAS; Sofia, Akad. G. Bonchev St., Bl. 103B

Author: INA BORISLAVOVA ANASTASOVA

Dissertation title: Electrospun hybrid materials based on poly(L-lactide-*co*-D,L-lactide) and chitosan derivatives with purposely tailored design for potential biomedical applications and photocatalytic water purification

The research presented in this dissertation was carried out at the Laboratory of Bioactive Polymers within the Scientific Department Polymeric Biomaterials at the Institute of Polymers – BAS, under the supervision of Prof. Dr. Olya Stoilova. This research is also part of the scientific activities of the Laboratory of Bioactive Polymers, related to the development of innovative hybrid polymer materials with purposely tailored design and targeted properties for potential applications in biomedicine and photocatalytic water purification.

Part of the research presented in this dissertation was carried out with the financial support of the Bulgarian National Science Fund (Grant КП-06-Н39/13), and equipment from the Distributed Research Infrastructure INFRAMAT, part of the National Roadmap of Bulgaria for Research Infrastructure and financially supported by the Ministry of Education and Science, was used, for which I express my gratitude.

I would like to express my sincere gratitude to my supervisors – Prof. Dr. Olya Stoilova and Prof. Dr. Milena Ignatova, for their support in the preparation, writing, and formatting of this dissertation. I highly appreciate their comprehensive assistance, the valuable advice and guidance I received, and the patience they have shown towards me.

I thank all colleagues from the Laboratory of Bioactive Polymers for their support, understanding, and friendly attitude.

I thank Assoc. Prof. Dr. Nadya Markova (Institute of Microbiology, BAS) for her assistance in conducting the microbiological studies, Asst. Prof. Rositsa Kukeva and Prof. Dr. Radostina Stoyanova (Institute of General and Inorganic Chemistry, BAS) for their help with the EPR spectroscopy analysis of the samples, as well as Assoc. Prof. Dr. Ani Georgieva and Prof. Dr. Reneta Toshkova (Institute of Experimental Morphology, Pathology and Anthropology with Museum, BAS) for their methodological assistance in studying the antitumor activity of the materials that we have obtained.

I also would like to thank my family for their encouragement and faith in my achievements.

LIST OF ABBREVIATIONS

PLDLLA - Poly(L-lactide-*co*-D,L-lactide)

Ch - Chitosan

8QCHO - 8-Hydroxyquinoline-2-carboxaldehyde

Ch-8Q - Schiff base of chitosan with 8-hydroxyquinoline-2-carboxaldehyde

COS - Chitosan oligosaccharide

QCOS - Quaternized *N,N,N*-trimethyl chitosan iodide

TFA - Trifluoroacetic acid

DCM - Dichloromethane

DMF - Dimethylformamide

HeLa - Cervical cancer cell lines

MCF-7 - Breast cancer cell lines

BALB/c 3T3 - Non-cancer mouse fibroblast cells

DPPH• - 2,2-diphenyl-1-picrylhydrazyl radical

ROP - Ring-opening polymerization

SEM - Scanning electron microscopy

ATR-FTIR - Attenuated total reflection Fourier transform IR-spectroscopy

XPS - X-ray photoelectron spectroscopy

DSC - Differential scanning calorimetry

EPR - Electron paramagnetic resonance spectroscopy

EDX - Energy-dispersive X-ray spectroscopy

TGA - Thermogravimetric analysis

XRD - X-ray diffraction analysis

DAPI - 4′,6-diamidino-2-phenylindole

MTT - 3-(4,5-dimethylthiazol-2-yl)-2,5-diphenyltetrazolium bromide

AO - Acridine orange

EtBr - Ethidium bromide

INTRODUCTION

In recent years, electrospinning has been recognized as an effective technique for the fabrication of fibrous materials possessing a high specific surface area and a porous structure, which allows for the one-step incorporation of biologically active compounds and inorganic nanoparticles. These electrospun materials exhibit controlled release profiles of the active substances, enhanced therapeutic efficacy, and reduced toxicity, which makes them suitable candidates for local drug delivery and anti-tumor therapy, as well as for the photocatalytic degradation of organic pollutants in aqueous and atmospheric environments.

Biopolymers are among the most promising materials capable of replacing conventional plastics, whose extensive use leads to the accumulation of waste and the pollution of soils, water, and the atmosphere. Among them, poly(lactic acid) (PLA) and its copolymers stand out due to their biocompatibility, biodegradability, and good mechanical and physical properties. PLA has already found wide application in agriculture, the automotive industry, packaging production, and biomedicine, and its market share is expected to increase even further in the future. On the other hand, quaternized derivatives of the natural polysaccharide chitosan and its Schiff bases with 8-hydroxyquinoline derivatives exhibit low toxicity, biocompatibility, biodegradability, and inherent antibacterial properties, which are significantly enhanced by coordination with transition metal ions such as Cu^{2+} and Fe^{3+}.

Based on these considerations, the present dissertation focuses on two key aspects. The first concerns the development of novel fibrous materials designed for the local treatment of wounds and tumor diseases, based on poly(L-lactide-*co*-D,L-lactide) (PLDLLA) and the Schiff base of chitosan with 8-hydroxyquinoline derivatives, followed by their complexation with Cu^{2+} and Fe^{3+} ions. The second aspect involves the design of hybrid fibrous materials composed of PLDLLA, quaternized chitosan oligosaccharides, and ZnO and Fe_3O_4 nanoparticles with a purposely tailored design, exhibiting high antioxidant and photocatalytic activity, for the purification of waters contaminated with organic pollutants. These studies aim to bridge existing gaps

in the literature and propose a set of innovative materials with a broad range of biomedical and environmental applications.

II. AIM AND OBJECTIVES OF THE DISSERTATION

Based on the conclusions drawn from the state-of-the-art and the extensive experience of the Laboratory of Bioactive Polymers in the field of electrospinning and the development of biomaterials from natural and synthetic polymers for applications in biomedicine, agriculture, and environmental protection, the following aim of the dissertation has been formulated:

To fabricate and characterize electrospun hybrid materials based on poly(L-lactide-*co*-D,L-lactide) (PLDLLA) and chitosan derivatives with a purposely tailored design, and to demonstrate their potential applications in biomedicine as well as in the photocatalytic water purification.

To achieve this aim, the following **objectives** were set:

1. Synthesis and characterization of the chitosan Schiff base with 8-hydroxyquinoline-2-carboxaldehyde (Ch-8Q). Determination of the suitable conditions for the electrospinning of PLDLLA and Ch-8Q, followed by the preparation of complexes of the resulting fibrous materials with Cu^{2+} and Fe^{3+} ions.

2. Characterization of the obtained set of hybrid fibrous materials and investigation of their antibacterial and anticancer activities.

3. Fabrication of hybrid fibrous materials with different design from PLDLLA, a quaternized chitosan derivative, and ZnO and Fe_3O_4 nanoparticles by combining electrospinning with electrospraying techniques.

4. Characterization of the obtained set of hybrid fibrous materials and evaluation of their antioxidant and photocatalytic activities.

III. RESULTS AND DISCUSSION

CHAPTER 1. Hybrid fibrous materials based on poly(L-lactide-*co*-D,L-lactide), the chitosan Schiff base with 8-hydroxyquinoline-2-carboxaldehyde, and their complexes with Cu^{2+} and Fe^{3+} ions: Investigation of their antibacterial and anticancer activities.

In the present chapter, the fabrication and characterization of novel fibrous materials based on the Schiff base of chitosan with 8-hydroxyquinoline-2-carboxaldehyde (Ch-8Q) and poly(L-lactide-*co*-D,L-lactide) (PLDLLA) are presented. Their complexes with biologically relevant transition metal ions - iron (Fe^{3+}) and copper (Cu^{2+}) - were also prepared and characterized. The morphology of the fibrous materials and their surface chemical composition were investigated using scanning electron microscopy (SEM), attenuated total reflection Fourier transform infrared spectroscopy (ATR-FTIR), and X-ray photoelectron spectroscopy (XPS). Their thermal properties were determined using differential scanning calorimetry (DSC). To study the coordination of metal ions (Cu^{2+} or Fe^{3+}) in the obtained fibrous materials, electron paramagnetic resonance (EPR) spectroscopy was employed. Considering the potential biomedical applications of the developed fibrous materials and their complexes, their antibacterial activity against pathogenic microorganisms (Gram-positive bacteria *S. aureus*) and their anticancer activity against human cancer cell lines (HeLa and MCF-7) were also evaluated.

Fabrication of hybrid fibrous materials based on poly(L-lactide-co-D,L-lactide), the chitosan Schiff base with 8-hydroxyquinoline-2-carboxaldehyde, and their complexes with Cu^{2+} and Fe^{3+} ions by electrospinning

The first step in the preparation of the hybrid fibrous materials was the synthesis of the chitosan Schiff base (Ch) with 8-hydroxyquinoline-2-carboxaldehyde (8QCHO). This Schiff base (Ch-8Q), reported here for the first time in the literature and within the scope of the present dissertation, was synthesized by modifying chitosan in an acetic acid aqueous medium with 8QCHO in an ethanol solution under mild conditions (Figure 1). The reaction product (Ch-8Q) was purified from the unreacted aldehyde by Soxhlet extraction with absolute ethanol and was isolated with a yield of 90%. Analysis of the ^{1}H NMR spectrum of the Schiff base indicated a degree of substitution of 73%.

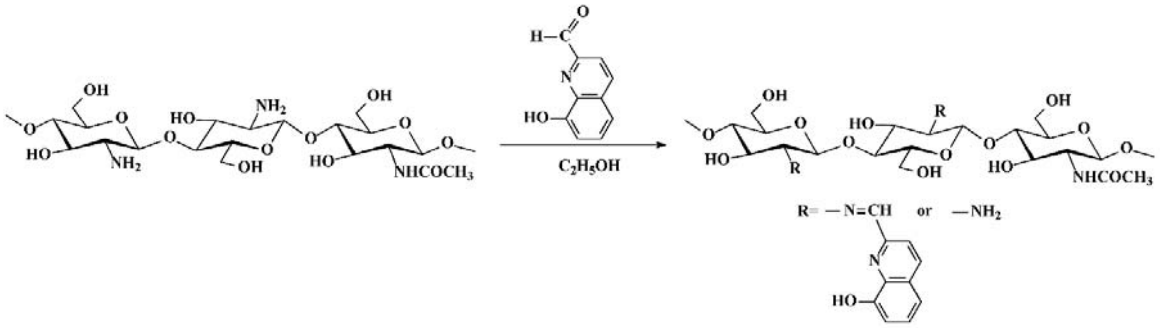

Figure 1. Scheme of the Synthesis of the Chitosan Schiff Base with 8-Hydroxyquinoline-2-Carboxaldehyde

The next step in the preparation of the hybrid fibrous materials was the optimization of the electrospinning parameters to obtain uniform and defect-free fibers. Trifluoroacetic acid (TFA) was selected as a common solvent for PLDLLA and the Schiff base, enabling the successful preparation of mixed spinning solutions. By varying the PLDLLA concentration, the weight ratio between PLDLLA and Ch-8Q, and the electrospinning parameters (applied voltage, distance between the capillary and collector, and solution feed rate), the following optimal conditions were established for producing defect-free and cylindrical PLDLLA/Ch-8Q fibers: PLDLLA:Ch-8Q weight ratios of 50:50 and 70:30, total polymer concentration of 5 wt.%, solution feed rate of 1 ml/h, and applied electric field intensity of 2.3 kV/cm. For comparison, fibrous materials from neat PLDLLA and from PLDLLA/Ch were also prepared under the same conditions.

Dynamic viscosity measurements of the spinning solutions showed that neat PLDLLA exhibited the highest viscosity (4200 cP), which decreased upon the addition of chitosan (1900 cP) and decreased further with the incorporation of the Ch-8Q Schiff base (1700 cP). The lowest viscosity values were observed for the PLDLLA/Ch-8Q 50:50 weight ratio (940 cP). Since the mats obtained from this solution were found to be too brittle for biological experiments, the PLDLLA/Ch-8Q 70:30 weight ratio was selected for subsequent studies, providing good processability and mechanical stability of the fibers.

After determining the optimal electrospinning conditions and obtaining a set of mats with different compositions, the next step involved complexation with biologically relevant transition metal ions (Cu^{2+} and Fe^{3+}). This approach not only preserved the morphological characteristics of the mats but also

imparted to them additional biological properties. The complexes were formed by immersing the PLDLLA/Ch and PLDLLA/Ch-8Q mats in ethanolic solutions of the respective metal salts ($CuCl_2$ and $FeCl_3$) under controlled conditions. The presence of the metal ions and their coordination with chitosan and the Schiff base were subsequently confirmed by electron paramagnetic resonance (EPR) spectroscopy.

Morphological, structural, and physicochemical characterization of the obtained hybrid fibrous materials

The morphology of the obtained set of hybrid fibrous materials was examined using scanning electron microscopy (SEM) and is presented in Figure 2. It is noteworthy that electrospinning of PLDLLA resulted in the formation of uniform and homogeneous fibers (Figure 2a). In the mats composed of PLDLLA/Ch and PLDLLA/Ch-8Q, however, the formation of thin fibers originating from the main fibers was also observed (Figures 2b–d). These observations are consistent with previously reported results for mats of Ch and PLDLLA/Ch by other authors and are most likely attributed to jet stretching processes and to the rapid evaporation of the TFA solvent. These factors lead to changes in the shape and charge distribution along the jet, which in turn alters the balance between the surface tension and the electrostatic forces. As a result, partial jet splitting and fiber branching occur, which explains the observed morphology. After complexation with Cu^{2+} and Fe^{3+} ions, the PLDLLA/Ch-8Q mats retained both their fibrous structure and their characteristic morphology (Figures 2e,f). This indicates that the coordination of metal ions does not affect fiber integrity and does not alter fiber morphology, which is crucial for maintaining their functional properties and potential biomedical applications.

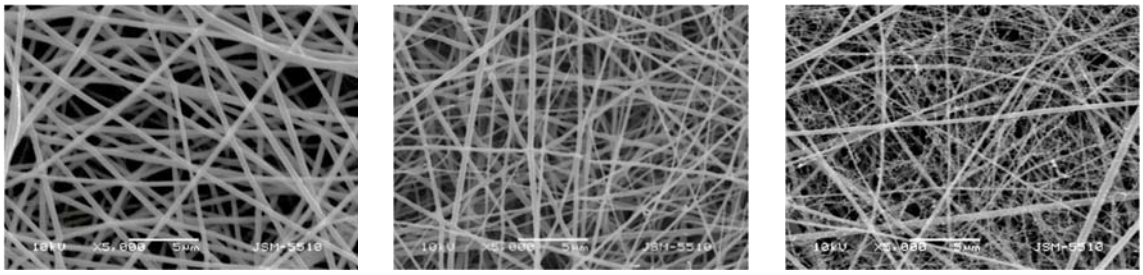

a **b** **c**

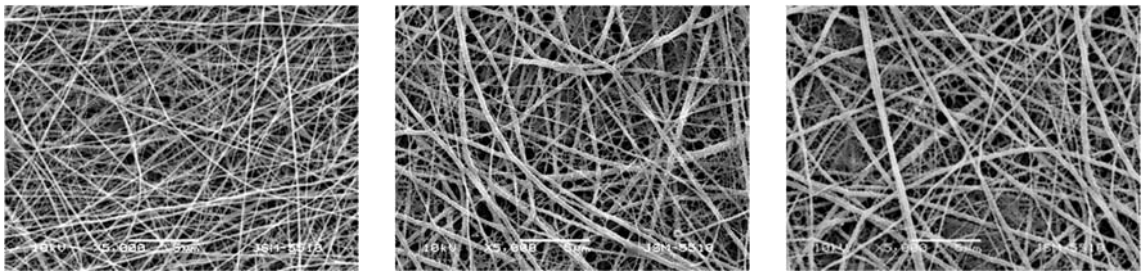

d **e** **f**

Figure 2. SEM micrographs of electrospun mats of: PLDLLA (**a**), PLDLLA/Ch (**b**), PLDLLA/Ch-8Q (70:30) (**c**), PLDLLA/Ch-8Q (50:50) (**d**), Cu^{2+}-PLDLLA/Ch-8Q (**e**) and Fe^{3+}-PLDLLA/Ch-8Q (**f**).

The measured average fiber diameters showed a clear dependence on the composition of the spinning solutions. Fibers from neat PLDLLA exhibited an average diameter of 360 ± 90 nm. Upon addition of chitosan to the PLDLLA solution, the average diameter decreased to 238 ± 105 nm, which correlates with the lower dynamic viscosity of the solution. The smallest average diameter was observed for fibers from PLDLLA/Ch-8Q (70:30) – 187 ± 128 nm. This reduction correlates with the measured lower solution viscosities in the following order: PLDLLA (4200 cP) > PLDLLA/Ch (1900 cP) > PLDLLA/Ch-8Q (1700 cP). Fibers from PLDLLA/Ch and PLDLLA/Ch-8Q exhibited a broader diameter distribution compared to neat PLDLLA, which explains the higher standard deviation values. This is likely due to the different ionic nature of the polymer systems, which affects the jet stability during electrospinning and the thinning processes during fiber formation. After complexation with Cu^{2+} and Fe^{3+} ions, the average fiber diameter remains practically unchanged – 208 ± 126 nm for the Cu^{2+} complex and 189 ± 130 nm for the Fe^{3+}complex. This confirms that the treatment of the mats with metal ions does not alter the structural characteristics of the materials.

To confirm the chemical composition of the PLDLLA/Ch-8Q mats and to monitor the complex formation with Cu^{2+} and Fe^{3+}, ATR-FTIR spectroscopy was used. In the spectrum of the PLDLLA/Ch mats, both the characteristic PLDLLA bands at 1751 cm^{-1} (νC=O) and 1084 cm^{-1} (νC–O), and those of chitosan - at 1676 cm^{-1} (νNH_3^+), 1558 cm^{-1} (amide II), and 3348 cm^{-1} (νO–H/νN–H) - can be observed. In the spectrum of the PLDLLA/Ch-8Q mats, in addition to the PLDLLA bands, characteristic bands at 1664 cm^{-1} (amide I), 1645 cm^{-1} (νC=N of the Schiff base), and 1506 cm^{-1} (νC=C of the aromatic ring

of 8Q) are also recorded, confirming the successful incorporation of Ch-8Q. It can be seen that after treating the PLDLLA/Ch-8Q mats with Cu^{2+} and Fe^{3+}, the band corresponding to νC=N of the azomethine group shifts from 1645 to 1622 cm^{-1}, indicating coordination with the nitrogen of the azomethine group in Ch-8Q. This shift is consistent with literature data for metal complexes of other Schiff bases. In addition, in the spectra of the complexes, the band assigned to νC=N from the 8Q residues in Ch-8Q, which appears at 1591 cm^{-1} in the spectrum of 8-hydroxyquinoline-2-carboxaldehyde, shifts to 1593 cm^{-1} (for the Cu^{2+}-PLDLLA/Ch-8Q mat) and to 1597 cm^{-1} (for the Fe^{3+}-PLDLLA/Ch-8Q mat), suggesting that the lone pair of electrons on the nitrogen of the 8Q residues participates in the coordination, similar to what has been described in the literature. A decrease in the intensity of the bands around 3340 cm^{-1} is also observed, which is likely related to the interaction of the metal ions with the –OH and $–NH_2$ groups. The observed changes in the spectra of the PLDLLA/Ch-8Q mats confirm the successful complex formation and are consistent with previous studies on metal complexes of Schiff bases.

The thermal properties of the PLDLLA/Ch-8Q mats and their complexes with Cu^{2+} and Fe^{3+} were investigated using DSC (Figure 3). In the thermograms of all samples containing Ch or Ch-8Q, a broad, weak endothermic peak between 25 - 100°C is observed, which is associated with the desorption of water or residual TFA (Figure 3b–e). The PLDLLA mats show a glass transition temperature (T_g), a cold crystallization temperature (T_{cc}), and a melting temperature (T_m) at 62°C, 89°C, and 153°C, respectively (Figure 3a). In the thermograms of the mats containing Ch and Ch-8Q, as well as in those of the complexes with Cu^{2+} and Fe^{3+}, the absence of T_{cc} indicates suppressed crystallization of PLDLLA as a result of blending and complex formation. The T_g of PLDLLA remains practically unchanged (≈ 61°C) for all types of mats (Figure 3b–e), which suggests that the incorporation of Ch-8Q and the metal ions does not affect the mobility of the polymer chains in the amorphous region. However, the T_m of PLDLLA shifts to lower values for PLDLLA/Ch, PLDLLA/Ch-8Q, and their complexes, confirming a change in the crystalline structure. As for Ch, no melting peak is detected for Ch-8Q (Figure 3b,c). At

temperatures above 280°C, endothermic signals associated with thermal degradation of the polymer components appear (Figure 3a–e).

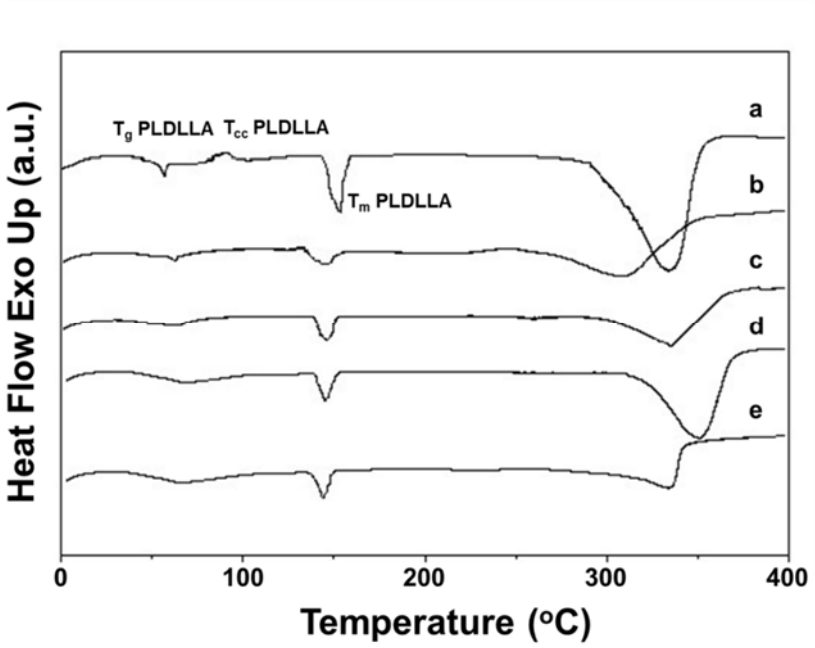

Figure 3. DSC thermograms of mats from: PLDLLA (**a**), PLDLLA/Ch (**b**), PLDLLA/Ch-8Q (**c**), Cu^{2+}-PLDLLA/Ch-8Q (**d**) и Fe^{3+}-PLDLLA/Ch-8Q (**e**).

The surface composition of the PLDLLA/Ch-8Q mats and their complexes with Cu^{2+} and Fe^{3+} was investigated using X-ray photoelectron spectroscopy (XPS), confirming the material structure and the successful incorporation of the Schiff base. In the C_{1s} spectrum of PLDLLA/Ch-8Q, signals corresponding to various functional groups are observed: at 285.0 eV - C–H and C–C bonds from PLDLLA and Ch-8Q, as well as C–NH_2; at 285.6 eV - C–N and C–OH bonds attributed to 8Q; at 286.8 eV - C–O, C–OH, and C–N–C=O from Ch-8Q, as well as C–O from PLDLLA, and C=N; at 288.4 eV - O–C–O and N–C=O from Ch-8Q; at 289.1 eV O–C=O from PLDLLA is detected; and at 290.5 eV - a $\pi \rightarrow \pi^*$ satellite signal characteristic of the aromatic ring of 8Q is detected. In the O_{1s} spectrum, four main components can be distinguished. The peak at 530.8 eV corresponds to N–C=O groups in Ch-8Q, while that at 532.2 eV reflects C=O groups from PLDLLA. The component at 532.9 eV arises from C–OH groups in Ch-8Q and 8Q, and the peak at 533.5 eV is attributed to O–C–O and C–O bonds characteristic of PLDLLA. The N_{1s} signal contains four well-defined peaks: at 398.8 eV, corresponding to N=C in Ch-8Q; at 399.6 eV, assigned to N–C=O and C–NH_2; at 400.8 eV, characteristic

of N–C from the 8Q moieties; and at 401.8 eV, reflecting protonated $–NH_3^+$ groups from chitosan. The theoretically estimated and experimentally obtained peak area ratios corresponding to the various types of carbon atoms - [C–C/C–H/C–NH_2], [C–N/C–OH], [C–O/C–OH/C–N–C=O/C–O/C=N], [O–C–O/N–C=O], [O–C=O]/[π→π*] showed very close agreement, with theoretical values of 34.1/2.3/36.1/3.5/23.3/0.7 and experimental values of 35.5/2.3/35.3/3.4/22.8/0.7. The dominant contribution arises from carbon atoms involved in C–C, C–H, and C–NH_2 bonds, which correlates well with the hydrophobic character observed on the mat surfaces.

In the high-resolution C_{1s} spectra of the PLDLLA/Ch-8Q mat complexes with Cu^{2+} and Fe^{3+} ions, a new component appears at 287.2 eV, characteristic of C–O–Cu/C–N–Cu or C–O–Fe/C–N–Fe type bonds. Concurrently, a decrease in the intensity of the peak at 286.8 eV is observed. In the O_{1s} spectra of these complexes, an additional signal at 531.2 eV is detected, attributed to O–Cu or O–Fe coordination originating from the 8Q residues in Ch-8Q. Similarly, the N_{1s} spectra exhibit an additional peak at 400.1 eV, corresponding to C–N–Cu or C–N–Fe interactions.

The complexation with Cu^{2+} ions is further confirmed by the presence of a Cu_{2p} signal composed of two components— $Cu_{2p1/2}$ and $Cu_{2p3/2}$. The $Cu_{2p3/2}$ peak exhibits a main maximum at 933.7 eV and two satellite peaks at 940.9 eV and 944.6 eV. The binding energy of the main peak correlates very well with values for Cu^{2+} complexes reported in the literature (933.1 eV). In the XPS spectrum of the Fe^{3+} complex, a new $Fe_{2p3/2}$ signal appears with a main peak at 711.9 eV and a satellite at 718.2 eV, consistent with values characteristic of Fe^{3+} complexes. These results clearly confirm the coordination of Cu^{2+} or Fe^{3+} ions on the surface of the PLDLLA/Ch-8Q fibrous materials.

Electron paramagnetic resonance (EPR) spectroscopy was employed to elucidate the coordination mechanism of Cu^{2+} and Fe^{3+} ions in the complexes of the PLDLLA/Ch-8Q mats. As reference materials, complexes of Cu^{2+} and Fe^{3+} ions with PLDLLA/Ch mats, as well as Cu^{2+} complexes with Ch-8Q and Fe^{3+} complexes with 8QCHO in the solid state, were analyzed. All samples were investigated within the temperature range of 100 - 295 K.

The EPR spectrum of the Cu^{2+} complex in the PLDLLA/Ch-8Q mats exhibits an almost symmetric signal with slightly resolved $g_{\perp}$ = 2.10 and $g_{II} \approx 2.26$ (Figure 4a). Its shape and position remain unchanged upon cooling, although the intensity increases following the Curie–Weiss law ($\theta = -147 \pm 6$ K). These parameters are characteristic of magnetically coupled Cu^{2+} ions. Since Ch-8Q is a derivative of Ch with 8QCHO, coordination of Cu^{2+} ions may occur both with the 8Q moieties and with Ch. To determine the actual coordination environment, two models were compared: coordination of Cu^{2+} in PLDLLA/Ch mats and coordination of Cu^{2+} with Ch-8Q in the solid state. The EPR spectrum of Cu^{2+}-PLDLLA/Ch (Figure 4b) displays a symmetric signal with g = 2.133, which remains constant over the temperature range 100–295 K. The linewidth (ΔH_{pp}) varies from 22.8 mT at 295 K to 19.7 mT at 100 K, and the temperature dependence of the reciprocal signal intensity (1/I) follows the Curie–Weiss law ($\theta = -28 \pm 7$ K). These parameters are characteristic of exchanged coupled Cu^{2+} ions. The observed g-value is close to that reported by Pawlicka et al. for Ch membranes with Cu^{2+} (g_{av} = 2.123), indicating coordination of Cu^{2+} ions with Ch in the Cu^{2+}-PLDLLA/Ch mats.

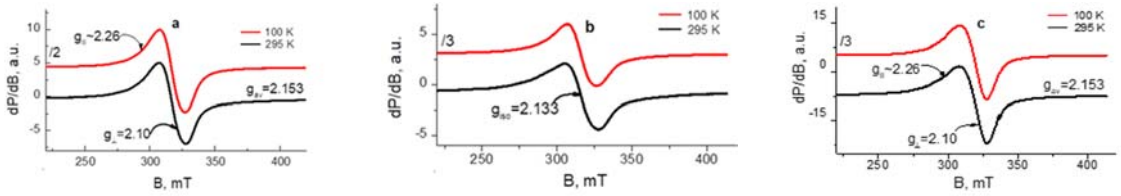

Figure 4. EPR spectra at 100 K and 295 K of mats from Cu^{2+}-PLDLLA/Ch-8Q (a) and Cu^{2+}-PLDLLA/Ch (b), and of Cu^{2+}-Ch-8Q in the solid state (c).

In the spectrum of the Cu^{2+}-Ch-8Q complex in the solid state (Figure 4c), a slightly asymmetric signal with low intensity and partially resolved hyperfine lines is observed. At 295 K, the Cu^{2+}-PLDLLA/Ch-8Q complex exhibits $g_{II} \approx 2.26$, $g_{\perp} \approx 2.10$ and g_{av} = 2.153. Upon cooling, the asymmetry decreases, and the temperature dependence of the signal intensity follows the Curie–Weiss law ($\theta = -52 \pm 4$ K). The g_{av} value of the Cu^{2+}-Ch-8Q complex is close to the g_{iso} of the Cu^{2+}-8Q complex, but different from that of the Cu^{2+}-PLDLLA/Ch complex, indicating coordination of Cu^{2+} with the 8Q moieties. The comparison of the Cu^{2+}-PLDLLA/Ch-8Q complex parameters with the reference samples reveals two key observations: (i) the g-value differs from that of the Cu^{2+}-

PLDLLA/Ch complex, and (ii) it is similar to that of the Cu^{2+}-Ch-8Q complex in the solid state. This demonstrates that the Cu^{2+} ions in the PLDLLA/Ch-8Q mats are coordinated primarily with the 8Q residues by O and N atoms.

The spectrum of the Fe^{3+} complex in the PLDLLA/Ch-8Q mats (Figure 5a) contains a broad, symmetric signal with g = 2.04 and $\Delta H_{pp} \approx 93$ mT at 295 K. For comparison, in the mats of the Fe^{3+}-PLDLLA/Ch complex (Figure 5b), two signals are observed with g ≈ 4.3 and g ≈ 2.0, with the component with g ≈ 4.3 being predominant. In contrast, in the mats of the Fe^{3+}-PLDLLA/Ch-8Q complex, the signal with g ≈ 2.0 dominates, and its intensity is more than 50 times higher than that of Fe^{3+}-PLDLLA/Ch. This indicates a significantly higher concentration of coordinated Fe^{3+} ions and suggests that the 8Q residues play a major role in the coordination of Fe^{3+} in the PLDLLA/Ch-8Q mats. To confirm this, the Fe^{3+}-8QCHO complex in the solid state was also investigated, showing a similar broad and symmetric signal with g = 2.06 and $\Delta H_{pp} \approx 100$ mT at 295 K. The similarity between the spectrum of this reference complex and that of the Fe^{3+}-PLDLLA/Ch-8Q mats supports the conclusion that the Fe^{3+} ions in the mats are predominantly coordinated with the 8Q residues of Ch-8Q.

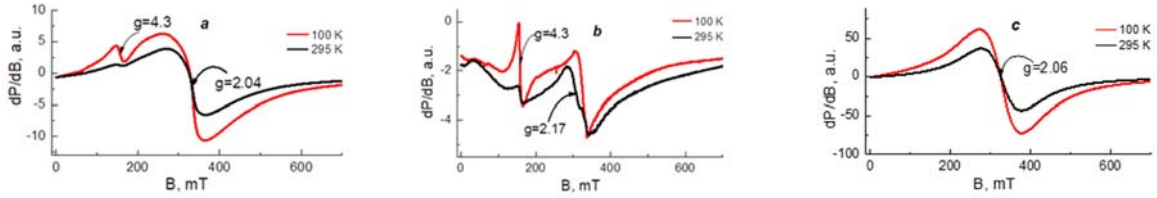

Figure 5. EPR spectra at 100 and 295 K of mats of Fe^{3+}-PLDLLA/Ch-8Q (a) and Fe^{3+}-PLDLLA/Ch (b), and of Fe^{3+}-8QCHO in the solid state (c).

It is well known that the cell adhesion and proliferation depend highly on the wettability of the surface of the electrospun materials. Therefore, the wettability of the surface of the obtained fibrous materials was measured, considering their contact with bacterial and cancer cells. It was found that the PLDLLA mat possesses a hydrophobic surface, with a water contact angle of 121.4° ± 2.0° (Figure 6a), where the water droplet retains its spherical shape on the surface of the mat. The incorporation of Ch into the PLDLLA fibers results in significant hydrophilization - the contact angle decreases to 50.2° ± 5.3° (Figure 6b). The PLDLLA/Ch-8Q mats remain hydrophobic, with a contact angle of 112.9° ± 5.6° (Figure 6c). Notably, the coordination of Cu^{2+} and Fe^{3+}

ions with these mats leads to a significant increase in the wettability, with the contact angle decreasing to approximately 78° (Figure 6d,e). This indicates that the metal ions exert a pronounced hydrophilizing effect on the surface properties of the fibrous materials.

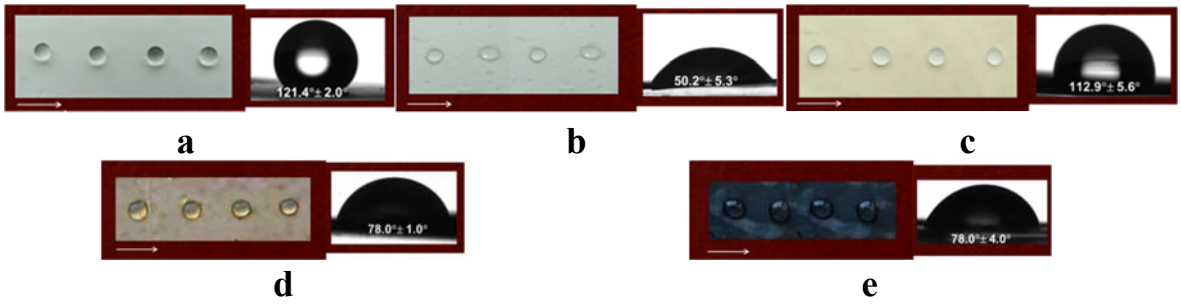

Figure 6. Digital images of the water contact angle for mats of: PLDLLA (**a**), PLDLLA/Ch (**b**), PLDLLA/Ch-8Q (**c**), Cu^{2+}-PLDLLA/Ch-8Q (**d**) и Fe^{3+}-PLDLLA/Ch-8Q (**e**). The direction of the collector rotation is indicated by an arrow.

The successful fabrication and characterization of the hybrid fibrous materials demonstrated that their morphology and physical properties make them suitable for biomedical applications. Despite these positive results, one of the key requirements for biomedical use remains the biocompatibility and the safety for the living cells. Therefore, the next step in the research focuses on evaluating the biological properties of the fibrous materials, including their ability to inhibit microbial growth and their potential impact on the viability of various cell lines. In addition, a detailed analysis of cell death was conducted to identify any possible cytotoxic effects. The obtained data will provide a comprehensive understanding of the safety and the potential applications of the hybrid fibrous materials in the biomedicine.

Biological properties of the fibrous materials: Antibacterial activity, cytotoxicity, and cell death analysis

The antibacterial activity of the mats composed of PLDLLA, PLDLLA/Ch, PLDLLA/Ch-8Q, and their complexes with Cu^{2+} and Fe^{3+} was evaluated against the Gram-positive bacteria *S. aureus* by counting the viable bacteria in the suspension after incubating the mats for different time periods. These bacteria were chosen due to their high prevalence as pathogenic microorganisms responsible for secondary infections in wounds.

The *S. aureus* control exhibited normal growth for the given time periods in the experiment, with log(CFU/mL) reaching 13.4 after 24 hours. As shown in Figure 7, the PLDLLA mats did not inhibit the growth of *S. aureus*, with the number of viable cells reaching 13.0 log after 24 hours. In contrast, the PLDLLA/Ch mats reduced the *S. aureus* titer to 7.2 log after 24 hours of contact (Figure 7). Notably, in the case of the PLDLLA/Ch-8Q mats, the *S. aureus* titer decreased to 2 log after just 2 hours of contact, whereas for the Cu^{2+} and Fe^{3+} complexes, the titer dropped to 1 and 0.9 log, respectively, for the same contact time (Figure 7). After 3 hours of contact with the PLDLLA/Ch-8Q mats and their complexes with Cu^{2+} and Fe^{3+}, no viable *S. aureus* cells were detected. These results indicate that the incorporation of Ch-8Q into the mats, as well as the formation of complexes with Cu^{2+} and Fe^{3+}, significantly enhances the antibacterial activity compared to that of the PLDLLA/Ch mats. The mats containing Ch-8Q and their complexes exert their antibacterial effect through direct contact with the bacteria, making them promising candidates for application as dressings for infected wounds.

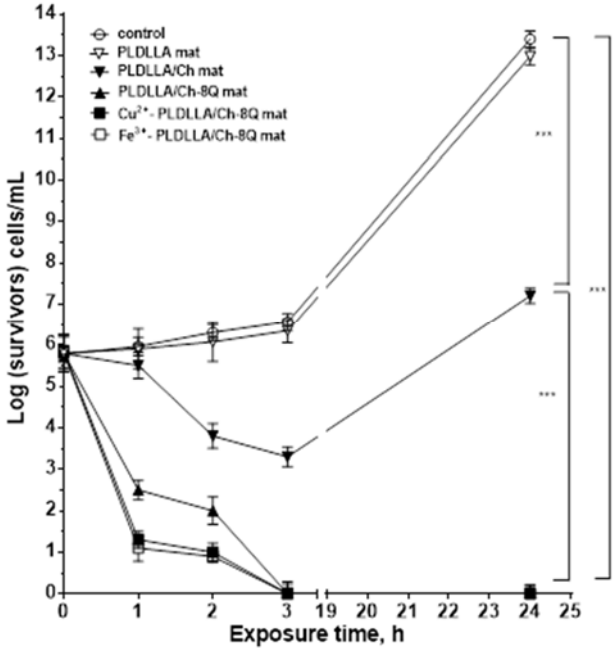

Figure 7. Logarithmic plot of the viable bacterial cell *S. aureus* number versus the exposure time for: the control (*S. aureus*), PLDLLA, PLDLLA/Ch, PLDLLA/Ch-8Q, and the PLDLLA/Ch-8Q complexes with Cu^{2+} and Fe^{3+}. Data are presented as mean ± standard deviation (n = 3); *** $p < 0.001$.

To evaluate the interaction of bacteria with the surfaces of the mats, the adhesion of *S. aureus* cells was observed using SEM. Figure 8 shows SEM micrographs of *S. aureus* cells adhered to the mat surfaces after 24 hours of contact with the suspension at 37°C. It can be seen that the cells adhere well on the hydrophobic PLDLLA mat and tend to form a biofilm (Figure 8a). In the PLDLLA/Ch mats, the number of adhered cells decreases, most likely due to the presence of Ch and its inherent antibacterial activity (Figure 8b). The incorporation of Ch-8Q into the fibers, as well as the formation of complexes with Cu^{2+} and Fe^{3+}, lead to complete inhibition of *S. aureus* growth on the mat surfaces (Figure 8c–e). These results indicate that the high bactericidal activity of the mats is due to the incorporated Ch-8Q and the complexation with Cu^{2+} and Fe^{3+} ions, making the mats promising materials for biomedical applications.

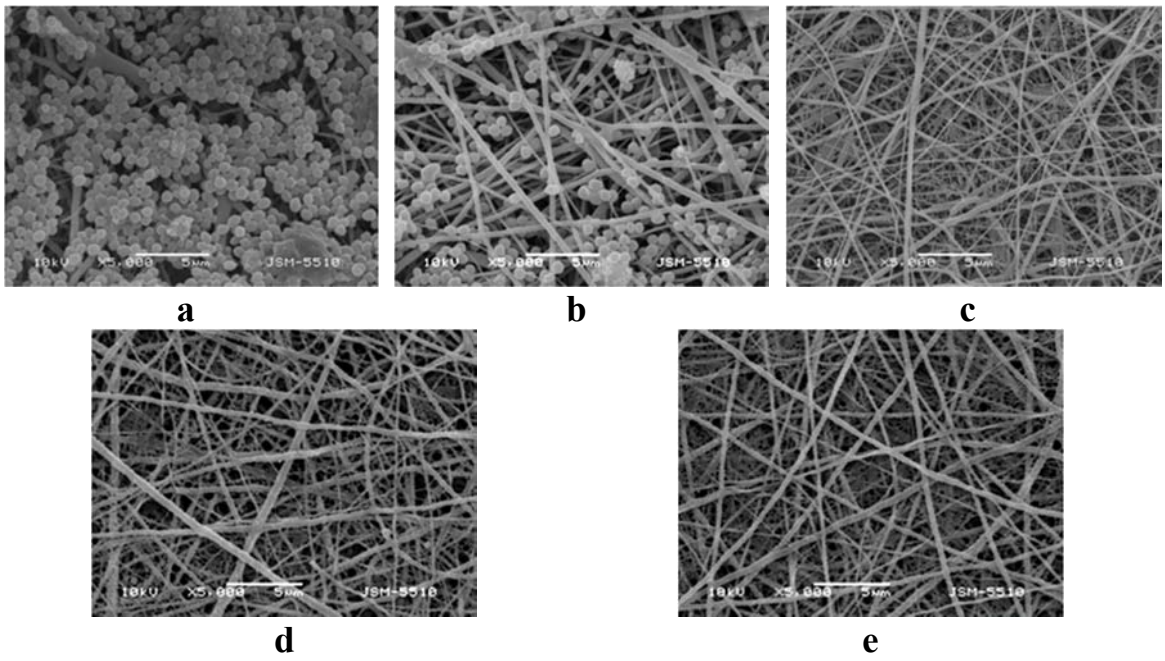

Figure 8. SEM micrographs of mats that have been incubated in *S. aureus* cell culture: PLDLLA (**a**), PLDLLA/Ch (**b**), PLDLLA/Ch-8Q (**c**), Cu^{2+}-PLDLLA/Ch-8Q (**d**) и Fe^{3+}-PLDLLA/Ch-8Q (**e**).

After confirming the high antibacterial activity of the PLDLLA/Ch-8Q mats and their complexes with Cu^{2+} and Fe^{3+}, the next step was to evaluate their effect on the viability and proliferation of cancer and normal cells *in vitro*.

It is known that 8QCHO exhibits strong antiproliferative activity against various human cancer cell lines, including Hs578t, SaoS2, K562, MDA231, SKHep1, T-47D, and Hep3B. Therefore, the viability of MCF-7 and HeLa cancer cells cultured in the presence of PLDLLA/Ch-8Q fibrous materials and

their complexes with Cu^{2+} and Fe^{3+} was evaluated *in vitro* using the MTT assay. The cytotoxic effect of these materials on non-cancer BALB/c 3T3 mouse fibroblast cells was also assessed.

The conducted studies showed that the PLDLLA and PLDLLA/Ch mats reduced the viability of the cancer cells only slightly (Figure 9a–d). In contrast, the presence of the PLDLLA/Ch-8Q mats and their complexes with Cu^{2+} and Fe^{3+} significantly decreased the viability of MCF-7 and HeLa cells, with the antiproliferative effect increasing with the duration of the incubation period. The highest cytotoxicity of the PLDLLA/Ch-8Q mats and their Cu^{2+} and Fe^{3+} complexes was observed after 72 hours (Figure 9b,d). It was found that the antiproliferative effect was more pronounced against HeLa cells compared to MCF-7 cells. After 72 hours, the Cu^{2+} and Fe^{3+} complexes of PLDLLA/Ch-8Q mats exhibited higher cytotoxicity against HeLa cells (2.6 ± 1.8% and 0.8 ± 0.7% viable cells, respectively) compared to the mats containing only Ch-8Q (27.4 ± 2.1% viable cells). In the case of MCF-7 cells, the Cu^{2+} complexes of PLDLLA/Ch-8Q caused a stronger reduction in proliferative activity (1.2 ± 1.3% viable cells) compared to the PLDLLA/Ch-8Q mats (48.6 ± 8.5%) and their Fe^{3+} complexes (34.0 ± 6.6%). In the case of non-cancer BALB/c 3T3 cells (Figure 9e,f), the PLDLLA/Ch-8Q mats did not exhibit a statistically significant antiproliferative effect, with cell viability after 72 hours remaining 90.0 ± 12.2%. The PLDLLA and PLDLLA/Ch mats also exhibited low cytotoxicity toward BALB/c 3T3 cells. In the case of PLDLLA/Ch-8Q complexes with Cu^{2+} and Fe^{3+}, the decrease in BALB/c 3T3 cell viability was less pronounced compared to that observed in the two cancer cell lines (Figure 9e, f). After 72 hours, the percentage of viable BALB/c 3T3 cells was 35.3 ± 4.0% for the Fe^{3+} and 5.4 ± 3.7% for the Cu^{2+} complexes of the mats. These results indicate that the hybrid fibrous materials based on PLDLLA/Ch-8Q and their Cu^{2+} and Fe^{3+} complexes exhibit strong antitumor activity against HeLa and MCF-7 cells, while maintaining lower toxicity towards normal BALB/c 3T3 fibroblasts.

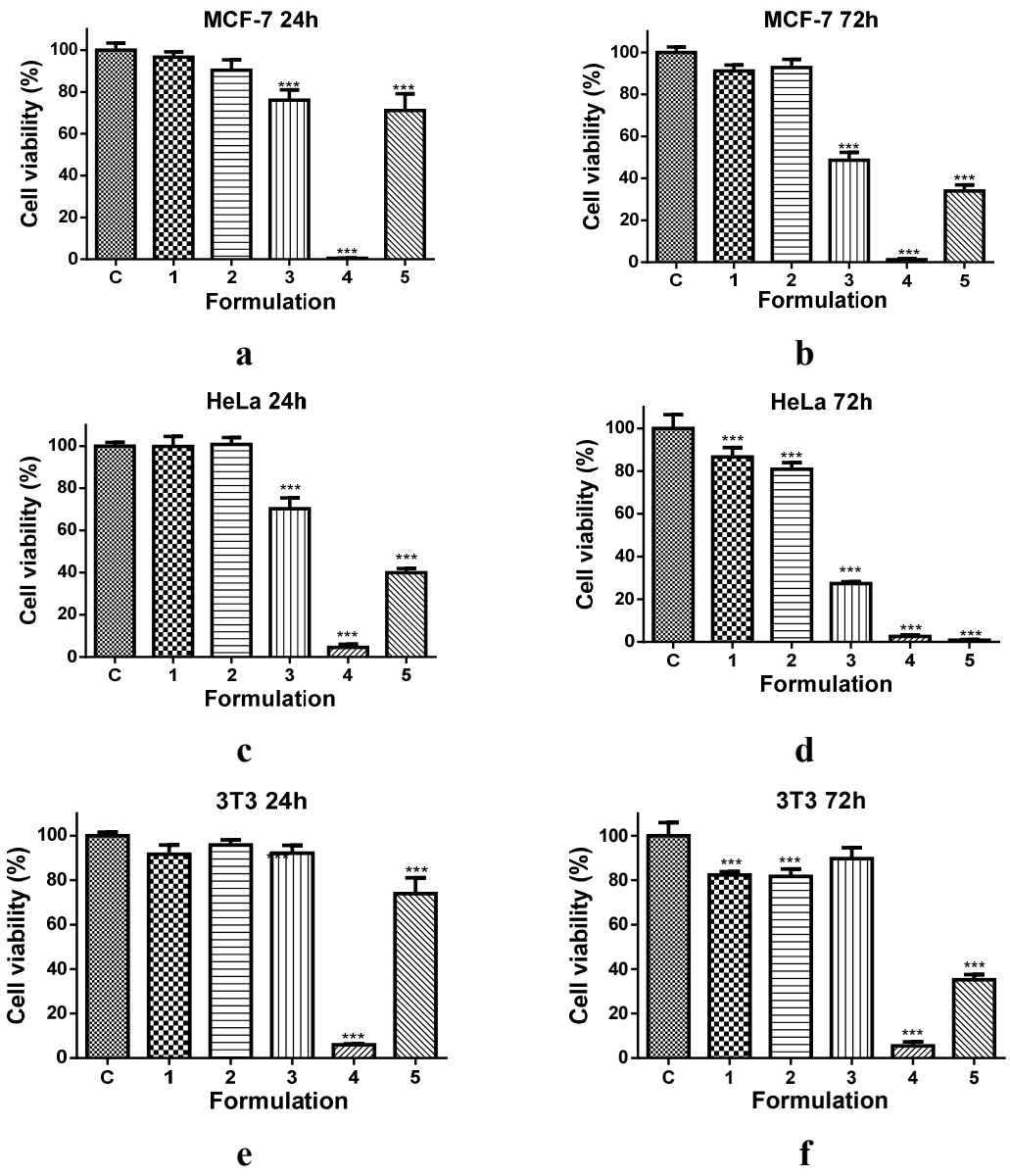

Figure 9. Effect of the different mats on the viability of MCF-7 (a,b), HeLa (c,d), and BALB/c 3T3 (e,f) cells after 24 h (a,c,e) and 72 h (b,d,f) of incubation. C – untreated cells (control); 1 – PLDLLA; 2 – PLDLLA/Ch; 3 – PLDLLA/Ch-8Q; 4 – Cu^{2+}-PLDLLA/Ch-8Q; 5 – Fe^{3+}-PLDLLA/Ch-8Q. ***$p < 0.001$.

To determine whether the antiproliferative effect of the fibrous mats containing Ch-8Q and their complexes with Cu^{2+} and Fe^{3+} is associated with the induction of apoptosis, a fluorescent cell death assay was performed using intravital double staining with acridine orange (AO) and ethidium bromide (EtBr). The morphological features of HeLa and MCF-7 cancer cells cultured for 24 hours in the presence of the different fibrous materials were examined. The untreated control cells were characterized by homogeneous pale-green

nuclei and bright yellow-green nucleoli. After treatment with PLDLLA and PLDLLA/Ch mats, no changes were observed in the morphology or staining of the nuclei and cytoplasm in HeLa and MCF-7 cells. The cells retained their normal structure. In the presence of PLDLLA/Ch-8Q mats and their complexes with Cu^{2+} and Fe^{3+}, characteristic apoptotic changes were observed, including cell rounding and cell shrinkage, cell membrane blebbing, cellular and nuclear volume reduction (pyknosis), condensation and aggregation of nuclear chromatin, the appearance of apoptotic bodies and nuclear fragmentation. These signs are characteristic of early and late apoptosis. The most pronounced morphological changes were observed after treatment with the Cu^{2+} complex of the PLDLLA/Ch-8Q mats. Numerous cells exhibiting red-orange staining of the nuclei and cytoplasm were observed, accompanied by a decrease in the number of viable cells and the presence of destructured cells with pyknotic nuclei - features typical of late apoptosis.

The morphological changes in the nuclei of HeLa and MCF-7 cells were also analyzed using DAPI staining. The results showed that the control, untreated cells had intact, oval-shaped nuclei of approximately equal size, with smooth edges and uniformly distributed chromatin. In the cells treated with PLDLLA and PLDLLA/Ch mats, the nuclear morphology remained similar to that of the control. However, in the cells treated with PLDLLA/Ch-8Q mats and their complexes with Cu^{2+} and Fe^{3+}, characteristic apoptotic changes were observed, including chromatin condensation, pyknosis, nuclear fragmentation, and the formation of apoptotic bodies. The most pronounced nuclear damage in both cell types was observed after treatment with the Cu^{2+} complex of the PLDLLA/Ch-8Q mats. These observations are consistent with the results obtained from the MTT assay and confirm that the Cu^{2+} and Fe^{3+} complexes of the PLDLLA/Ch-8Q mats exhibit strong antiproliferative activity against HeLa and MCF-7 cells, whereas the mats containing Ch-8Q show more moderate cytotoxicity. The fluorescence microscopy data clearly indicate that cell death occurs predominantly by the mechanism of apoptosis.

When normal BALB/c 3T3 mouse fibroblasts were cultured in the presence of the Cu^{2+} and Fe^{3+} complexes of the PLDLLA/Ch-8Q mats, morphological changes in the cells and nuclei characteristic of early and late

apoptosis were observed. These changes were most pronounced in the cells treated with the Cu^{2+} complex of the mats containing Ch-8Q, but were considerably weaker compared to those observed in HeLa and MCF-7 cancer cells. In contrast, the mats containing only Ch-8Q did not induce toxic effects on BALB/c 3T3 cells, confirming the higher selectivity of these materials towards tumor cells compared to normal fibroblasts.

In conclusion, the results from **Chapter 1** demonstrate that using electrospinning the optimal conditions for the one-pot preparation of novel fibrous materials based on PLDLLA and the newly synthesized chitosan Schiff base with 8-hydroxyquinoline-2-carboxaldehyde were found. Subsequent treatment of the PLDLLA/Ch-8Q mats with $CuCl_2$ or $FeCl_3$ solutions led to successful complex formation, yielding the corresponding Cu^{2+}-PLDLLA/Ch-8Q and Fe^{3+}-PLDLLA/Ch-8Q mats. The ATR-FTIR, XPS, and EPR analyses confirmed that in the fibrous structure, the metal ions are predominantly coordinated with the 8Q residues of Ch-8Q. It was demonstrated that the incorporation of Ch-8Q and the subsequent complexation with Cu^{2+} and Fe^{3+} impart to the mats pronounced antibacterial activity against the pathogenic bacteria *S. aureus*, as well as the ability to inhibit its adhesion. Furthermore, the fibrous mats from PLDLLA and Ch-8Q exhibit significant *in vitro* antitumor activity against human HeLa (cervical cancer) and MCF-7 (breast cancer) cells, while demonstrating no cytotoxicity towards normal BALB/c 3T3 mouse fibroblasts. Therefore, the obtained hybrid fibrous materials appear particularly promising for use as antibacterial dressings for infected wounds and as potential drug delivery carriers for the local treatment of cervical and breast cancers - diseases of high medical significance.

CHAPTER 2. Hybrid fibrous materials based on poly(L-lactide-*co*-D,L-lactide), quaternized chitosan oligosaccharide, and ZnO and Fe_3O_4 nanoparticles with a purposely tailored design. Investigation of their antioxidant and photocatalytic activities.

Water pollution from industrial sources is a serious global problem, for which heterogeneous photocatalysis offers a realistic and highly promising solution. In this context, hybrid polymeric materials with photocatalytic properties are considered particularly promising. Therefore, in the present

chapter, an original approach for the fabrication of a set of hybrid fibrous biomaterials with photocatalytic and magnetic properties is proposed by skillfully combining various easily implementable and effective methods: (i) electrospinning of a solution of poly(L-lactide-*co*-D,L-lactide) (PLDLLA) containing Fe_3O_4 nanoparticles, and (ii) simultaneous electrospinning of a PLDLLA or PLDLLA/Fe_3O_4 dispersion and electrospraying of a ZnO dispersion (widely used for heterogeneous photocatalysis under UV irradiation). The incorporation of Fe_3O_4 nanoparticles into PLDLLA fibers is an important step in the development of effective hybrid materials for water purification, which aimed at imparting magnetic properties to the materials and enabling their easy removal from the environment after use. An original solution for the efficient immobilization of the electrosprayed ZnO nanoparticles on the fiber surface is the addition of quaternized chitosan oligosaccharide (QCOS). The morphology of the materials was investigated using scanning electron microscopy (SEM) coupled with energy-dispersive X-ray spectroscopy (EDX) and transmission electron microscopy (TEM). The results from the thermogravimetric analysis (TGA) and the X-ray diffraction (XRD) indicate that the addition of inorganic particles affects the thermal properties and crystalline structure of the electrospun materials. For the first time, the antioxidant activity of fibrous materials containing ZnO was evaluated using the DPPH free radical scavenging assay, while the photocatalytic activity was monitored through the degradation of the model organic pollutant methylene blue under UV light irradiation.

Fabrication of hybrid fibrous materials based on poly(L-lactide-co-D,L-lactide), quaternized chitosan oligosaccharide, and ZnO and Fe_3O_4 nanoparticles with a purposely tailored design.

For the successful fabrication of the hybrid fibrous materials from PLDLLA, Fe_3O_4 and ZnO nanoparticles, it was first necessary to select a suitable solvent system to prepare the spinning solutions. Therefore, a mixed DCM/DMF solvent system was chosen, with DCM being preferred over the commonly used chloroform due to its higher vapor pressure, while DMF was added to increase the conductivity of the spinning solution and the charge density of the jet, in accordance with our previous studies. Preliminary

experiments were conducted to determine the optimal DCM/DMF ratio, the required PLDLLA concentration, and the optimal electrospinning parameters (applied voltage, solution feed rate, and needle-to-collector distance), all of which influence the morphology of the obtained fibers. Based on the obtained results, the optimal conditions for forming a stable Taylor cone (necessary for producing continuous and defect-free PLDLLA fibers) were established as follows: DCM/DMF ratio of 3:1 (v/v), PLDLLA concentration - 5% w/v, applied voltage - 20 kV, needle-to-collector distance - 20 cm, and solution feed rate - 2 mL/h. It should be noted that, until the fabrication of these materials, no data had been published on the use of this specific solvent system for the electrospinning of PLDLLA. Under the identified optimal conditions, the following set of hybrid fibrous materials was obtained (Scheme 1): materials of type "*in*", denoted as Fe_3O_4-*in*-PLDLLA, in which the nanoparticles are incorporated within the fiber volume; materials of type "*on*", denoted as ZnO/QCOS-*on*-PLDLLA, in which the nanoparticles are located on the fiber surface; and materials of type "*in-on*", denoted as ZnO/QCOS-*on*-(Fe_3O_4-*in*-PLDLLA), in which the nanoparticles are distributed both within the fiber's volume and on the fiber's surface.

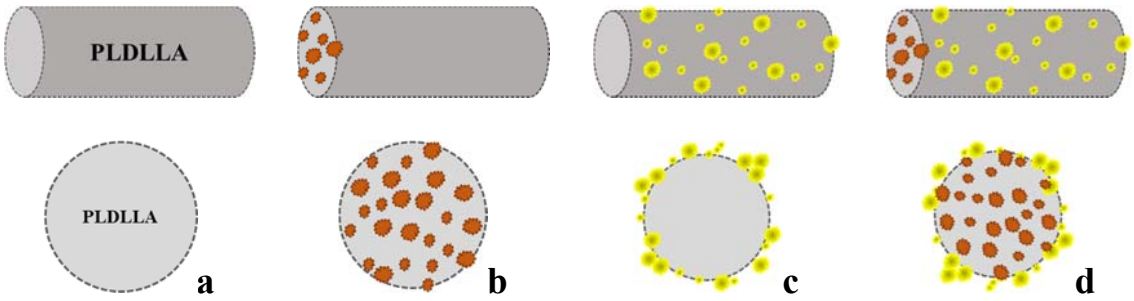

Scheme 1. Types of fibrous materials: (a) PLDLLA, (b) Fe_3O_4-*in*-PLDLLA, (c) ZnO/QCOS-*on*-PLDLLA and (d) ZnO/QCOS-*on*-(Fe_3O_4-*in*-PLDLLA).

The quaternized *N,N,N*-trimethyl chitosan iodide (QCOS), as a biodegradable, biocompatible, and water-soluble polymer with proven biological properties, was selected as a sticking agent for ZnO nanoparticles on the fibers. In addition, the preliminary experiments showed that QCOS is an excellent stabilizing agent for ZnO nanoparticle dispersions in water/ethanol (7/3 v/v). In this way, a set of hybrid fibrous materials with a purposely tailored design was obtained in a single step by electrospinning of PLDLLA or its blend

with Fe_3O_4 (Scheme 1 a,b), as well as by simultaneous electrospinning of PLDLLA or its blend with Fe_3O_4 and electrospraying of a ZnO/QCOS dispersion (Scheme 1 c,d).

Morphological, structural, and physicochemical characterization of the obtained hybrid fibrous materials.

The changes in the surface morphology of the obtained fibrous materials were observed using SEM (Figure 10). As expected, the electrospinning of PLDLLA resulted in the formation of monolith, cylindrical, and defect-free fibers (Figure 10a). The addition of the nanosized Fe_3O_4 to the PLDLLA spinning solution did not significantly change the morphology of the electrospun fibers, however, thicker parts along their length were observed, associated with the aggregation of some of the particles during the electrospinning process (Figure 10b). In contrast to the electrospun materials, those obtained by simultaneous electrospinning and electrospraying exhibited a distinct change in the morphology - deposition of ZnO particles or its aggregates on the surface of the fibers and along the length of the fibers (Figure 10c, d). A rough surface characteristic of fibers with design type "*on*" was observed, which is a result of the applied fabrication approach and is consistent with our previous studies.

From the SEM micrographs, the average fiber diameters and their distributions were measured. The average diameters of the PLDLLA and ZnO/QCOS-*on*-PLDLLA fibers were 1.12 ± 0.13 μm and 1.30 ± 0.17 μm, respectively. As expected, the diameters of Fe_3O_4-*in*-PLDLLA and ZnO/QCOS-*on*-(Fe_3O_4-*in*-PLDLLA) fibers were larger - 1.52 ± 0.25 μm and 1.53 ± 0.15 μm, respectively. Evidently, the incorporation of Fe_3O_4 into PLDLLA leads to a moderate increase in the average fiber diameter. The obtained SEM results confirm the proposed schematic representation of the different types of materials and demonstrate that fibrous materials with targeted design type "*in*", "*on*", and "*in-on*" can be successfully fabricated in a single step by electrospinning or by combining electrospinning with electrospraying (Scheme 1).

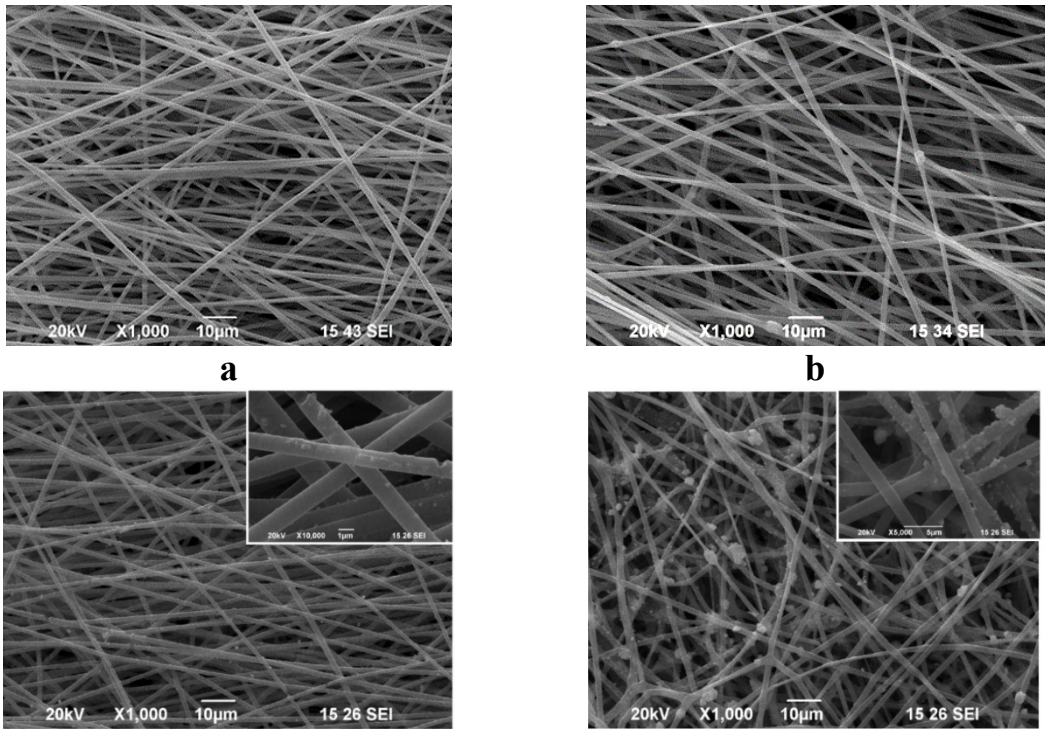

Figure 10. SEM micrographs (a–d) of the fibers from: PLDLLA (**a**), Fe_3O_4-*in*-PLDLLA (**b**), ZnO/QCOS-*on*-PLDLLA (**c**) and ZnO/QCOS-*on*-(Fe_3O_4-*in*-PLDLLA) (**d**).

The distribution of the Fe_3O_4 and ZnO particles was observed using TEM (Figure 11). It can be seen that the good homogenization of the Fe_3O_4 particles in the PLDLLA solution led to their almost uniform distribution along the length of the fibers during the electrospinning (Figure 11a). However, the formation of small aggregates was also observed, which was most likely due both to the rapid evaporation of the solvent system during the electrospinning and to the electrostatic attraction between the particles, regardless of their good dispersion (Figure 11a). During the simultaneous electrospinning of PLDLLA and electrospraying of ZnO/QCOS, a relatively uniform distribution of the ZnO particles on the fiber's surface was observed (Figure 11b). Moreover, the electrospraying process led to the enrichment of the fibers surface with ZnO and significantly increased their roughness. In this way, numerous active sites were created, allowing direct interaction with the polluted environment. In this way, as the surface area of the fibers increases, their ability to remove pollutants also improves. In the case of the combined electrospinning of Fe_3O_4/PLDLLA and electrospraying of ZnO/QCOS, both a uniform distribution of the particles along the fiber's length and their deposition on the fiber surface were observed

(Figure 11c). As clearly evident, the electrospraying also led to the formation of aggregates on the fiber's surface, similar to the electrospinning (Figure 11b, c). In this case, in addition to the rapid evaporation of the solvent, the addition of QCOS contributed to the sticking and aggregation of the particles. These observations are consistent with the results obtained from the SEM analysis and confirm that the targeted design of the fibrous materials can be successfully achieved in a single step by electrospinning or by combining it with electrospraying.

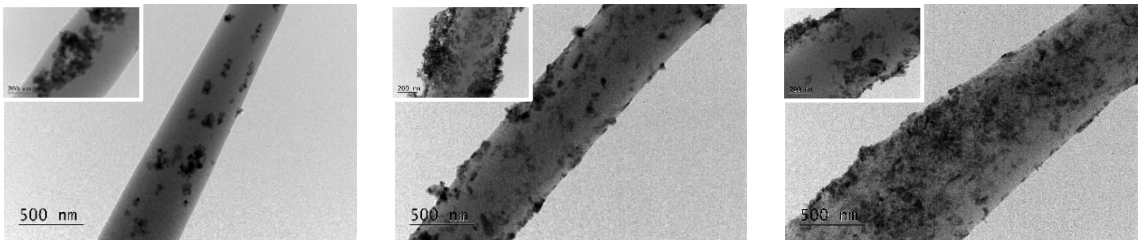

a **b** **c**

Figure 11. TEM micrographs of the fibrous materials: Fe_3O_4-*in*-PLDLLA (a), ZnO/QCOS-*on*-PLDLLA (b) и ZnO/QCOS-*on*-(Fe_3O_4-*in*-PLDLLA) (c).

Additional information on the distribution of the Fe_3O_4 and ZnO particles in the hybrid fibrous materials of ZnO/QCOS-*on*-(Fe_3O_4-*in*-PLDLLA) was obtained by energy-dispersive X-ray spectroscopy (EDX) (Figure 12). Elemental mapping performed by EDX revealed the presence of carbon, oxygen, iron, iodine, and zinc (Figure 12b–f), which was in full agreement with the TEM analysis, confirming the deposition of the Fe_3O_4 and ZnO particles along the fiber's length. It is noteworthy that the Fe_3O_4 particles were relatively well dispersed and formed smaller aggregates (Figure 12d) compared to the ZnO particles (Figure 12f). This was likely due to the different processes used for their incorporation into the fibers - electrospinning for Fe_3O_4 and electrospraying for ZnO - as well as the presence of QCOS (Figure 12e) in the ZnO dispersion.

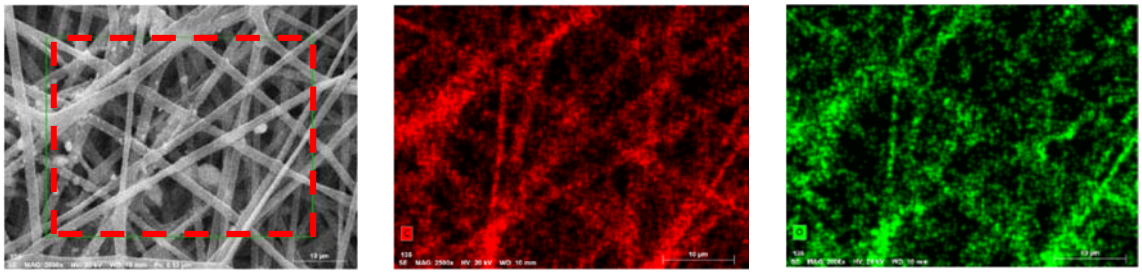

a **b** **c**

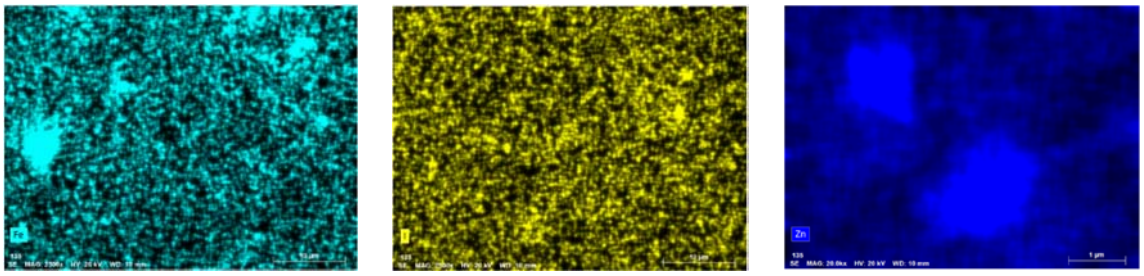

d **e** **f**

Figure 12. SEM-EDX analysis of hybrid fibrous materials from ZnO/QCOS-*on*-(Fe_3O_4-*in*-PLDLLA): SEM micrograph (**a**), elemental mapping of carbon (**b**), oxygen (**c**), iron (**d**), iodine (**e**), and zinc (**f**).

Morphological studies confirmed the presence of ZnO particles on the surface of the PLDLLA and Fe_3O_4-*in*-PLDLLA fibers. This intentional surface modification suggests also a change in the wettability of the fibrous materials. Indeed, it was found that the water contact angle of the fibrous materials decreases in the following order: PLDLLA (122.9°) > Fe_3O_4-*in*-PLDLLA (98.6°) > ZnO/QCOS-*on*-PLDLLA (26.2°) > ZnO/QCOS-*on*-(Fe_3O_4-*in*-PLDLLA) (0°). As expected, the water contact angle of the fibrous materials composed of PLDLLA and Fe_3O_4-*in*-PLDLLA was larger than 90°, due to the hydrophobic nature of PLDLLA. In contrast, the hybrid fibrous materials type "*on*" exhibited a water contact angle below 90°, confirming their hydrophilic character. This behavior was mainly attributed to the presence of both zinc oxide and QCOS. Thus, the surface wettability of the fibrous materials can be easily modified in one single step. Moreover, the increased wettability enhances the adsorption capacity and, consequently, this may facilitate the photocatalytic activity of the obtained fibrous materials.

After the morphological changes and surface properties of the fibrous materials were established, thermogravimetric analysis (TGA) was also performed to evaluate the influence of the inorganic particles (Fe_3O_4 and ZnO) on the thermal properties of the PLDLLA fibers. In addition, the amount of the incorporated inorganic components was also determined, confirming the efficiency of the proposed approach. The thermal degradation of the materials was studied in the temperature range from room temperature to 800 °C (Figure 13). As can be seen, the fibrous materials from PLDLLA and Fe_3O_4-*in*-PLDLLA undergo a one-stage decomposition, typical for polylactides, starting at 320°C and ending at 420°C, with maxima at 408°C and 363°C, respectively.

The PLDLLA fibers are completely decomposed, with a weight loss reaching nearly 100% at 800°C, whereas the hybrid fibers leave a residue of 9.9%. This residue is close to the amount of Fe_3O_4 added to the PLDLLA spinning solution and is attributed to the thermal stability of the inorganic component, which does not decompose in this temperature range. The materials ZnO/QCOS-*on*-PLDLLA and ZnO/QCOS-*on*-(Fe_3O_4-*in*-PLDLLA) exhibit two-step degradation. The first stage starts at 200°C and ends at 320°C with significant weight loss, while the second stage ends at 480°C (Figure 13). It is likely that the degradation steps of PLDLLA and QCOS overlap, with the corresponding weight losses of PLDLLA and QCOS being close to their theoretical values. Additionally, thermal degradation characteristic of polylactides in the presence of zinc compounds is also observed, which is consistent with literature reports. The degradation of the ZnO/QCOS-*on*-PLDLLA materials ends with a residue of 18.2%, while for ZnO/QCOS-*on*-(Fe_3O_4-*in*-PLDLLA) it reaches 28.1% (Figure 13). These residues most likely correspond to the amounts of ZnO and Fe_3O_4, as they are close to the initially added quantities in the dispersion and in the spinning solution. Additionally, ZnO and Fe_3O_4 do not decompose up to 800 °C. The reduced thermal stability of PLDLLA in the fibrous materials type "*on*" is likely due to both the known low thermal resistance of QCOS and the presence of ZnO.

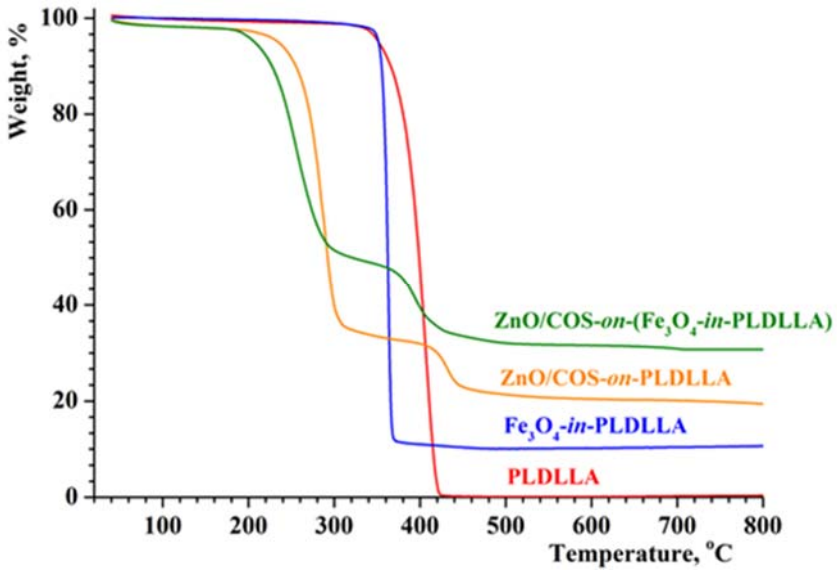

Figure 13. TGA curves of fibrous materials from PLDLLA, Fe_3O_4-*in*-PLDLLA, ZnO/QCOS-*on*-PLDLLA и ZnO/QCOS-*on*-(Fe_3O_4-*in*-PLDLLA).

In addition, the phase structures of the fibrous materials were further analyzed by X-ray diffraction (XRD). In the small-angle region (Figure 14), the presence of an amorphous halo in all fibrous materials is associated with the amorphous structure of PLDLLA. In particular, the rapid solidification of the fibers during the electrospinning process limits the spatial arrangement of the stretched polymer chains into ordered crystalline structures. The XRD patterns of the hybrid materials Fe_3O_4-*in*-PLDLLA, ZnO/QCOS-*on*-PLDLLA and ZnO/QCOS-*on*-(Fe_3O_4-*in*-PLDLLA) confirm the presence of the cubic phase of magnetite (PDF 89-0691) and the hexagonal phase of zinc oxide (PDF 36-1451). The crystalline phase of Fe_3O_4 is identified by peaks at 30.3° (220), 35.6° (311), 43.3° (400), 57.1° (511), and 62.8° (440), while that of ZnO shows peaks at 31.8° (100), 34.5° (002), 36.3° (101), 47.6° (102), 56.7° (110), 62.9° (103), 66.4° (200), 67.9° (112), and 69.2° (201). These well-defined reflexes indicate that the incorporation of Fe_3O_4 into the fibers and of ZnO onto the fiber surfaces does not affect the amorphous structure of PLDLLA. Moreover, the electrospinning and electrospraying processes do not influence the crystallinity of the inorganic particles.

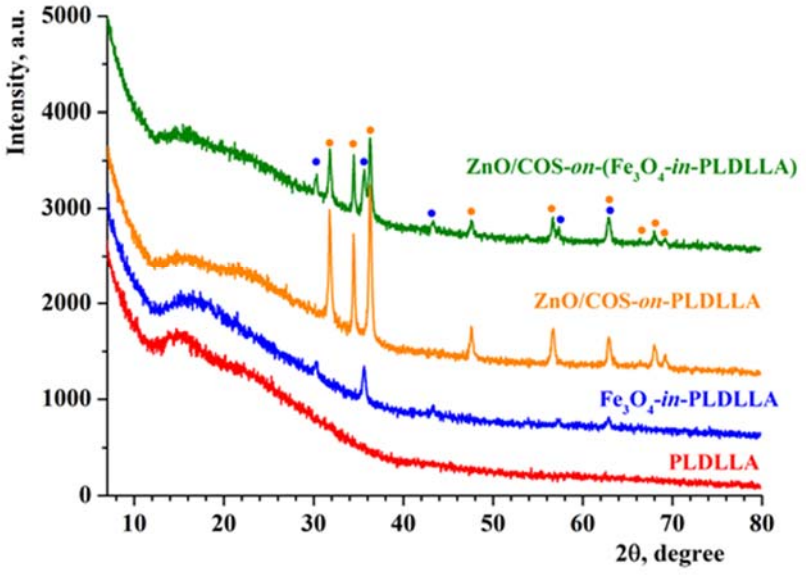

Figure 14. X-ray diffractograms of the fibrous materials from PLDLLA, Fe_3O_4-*in*-PLDLLA, ZnO/QCOS-*on*-PLDLLA и ZnO/QCOS-*on*-(Fe_3O_4-*in*-PLDLLA).

Imparting magnetic properties to the fibrous materials by adding Fe_3O_4 represents an effective approach for their easy removal from the reaction

medium under the application of an external magnetic field. Therefore, the saturated magnetization of the hybrid fibrous materials was measured using a vibrating sample magnetometer. The Fe_3O_4-*in*-PLDLLA materials exhibit higher magnetization (2.7 emu/g) than the ZnO/QCOS-*on*-(Fe_3O_4-*in*-PLDLLA) materials (below 1 emu/g), likely due to the lower amount of magnetic material incorporated in the latter. Consequently, the amount of Fe_3O_4 incorporated into the PLDLLA fibers is sufficient for the easy removal of the electrospun materials from the reaction medium under the action of a permanent magnet.

Antioxidant activity of the fibrous materials

After the detailed characterization of the morphology, structure, and physicochemical properties of the hybrid fibrous materials, their biologically relevant potential was also investigated by evaluating their antioxidant activity. It is well known that ZnO and QCOS possess antioxidant activity, which suggests the presence of such activity in the obtained fibrous materials. For the first time, the antioxidant activity of electrospun materials with purposely tailored design containing ZnO was examined using the DPPH radical-scavenging assay.

It was found that the materials of type "*on*" exhibit higher antioxidant activity compared to the materials of type "*in*" (Figure 15). After 30 minutes of contact time, the fibrous materials ZnO/QCOS-*on*-(Fe_3O_4-*in*-PLDLLA) and ZnO/QCOS-*on*-PLDLLA show DPPH• scavenging capacities of 76.0 ± 0.8% and 72.5 ± 0.2%, respectively. As can be seen in Figure 15, ZnO exhibits higher free-radical scavenging activity (60.2 ± 0.2%) compared to Fe_3O_4 (18.5 ± 0.1%) and QCOS (17.6 ± 0.3%). In contrast, the fibrous materials fabricated of PLDLLA exhibit the lowest antioxidant activity (3.9 ± 0.2%), while the incorporation of Fe_3O_4 into the fibers leads to a slight increase in their activity, approaching that of pristine Fe_3O_4 (Figure 15). Clearly, the ZnO particles deposited on the fiber surface act as electron acceptors that quench the DPPH radicals. On the other hand, the addition of QCOS exerts a synergistic effect on the action of ZnO, further enhancing the overall antioxidant activity and improving the efficiency of the fibrous materials of type "*on*".

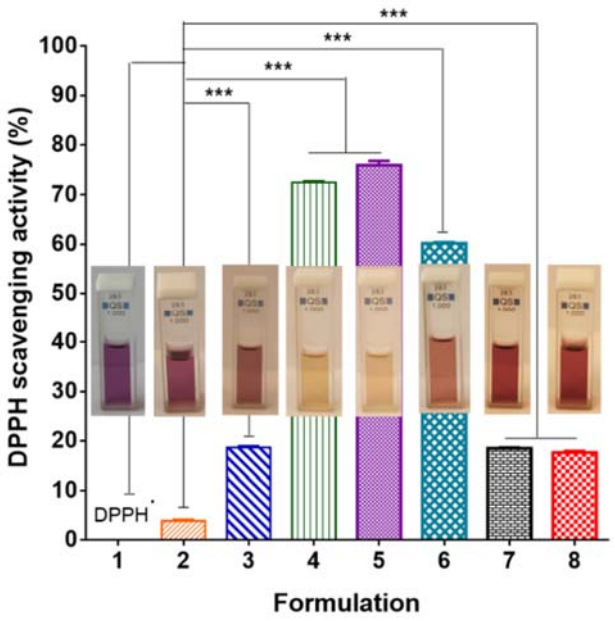

Figure 15. Antioxidant activity of fibrous materials: PLDLLA (2), Fe_3O_4-*in*-PLDLLA (3), ZnO/QCOS-*on*-PLDLLA (4) and ZnO/QCOS-*on*-(Fe_3O_4-*in*-PLDLLA) (5). Controls: DPPH• solution (1), ZnO (6), Fe_3O_4 (7), and QCOS (8). ***p < 0.001. Digital images of the corresponding solutions are also shown.

Photocatalytic activity and reusability of the fibrous materials

In addition to their large surface area, wettability, thermal and magnetic properties, and antioxidant activity, the obtained electrospun hybrid materials demonstrate high potential for use as environmentally friendly filtration membranes for long-term and large-scale water purification. Furthermore, the purposely tailored design and the high photocatalytic activity of the incorporated ZnO suggest that these materials will also possess significant photocatalytic activity.

Among organic dyes, methylene blue (MB) is a toxic, carcinogenic, and non-biodegradable compound and is one of the most widespread organic pollutants in water. Therefore, the photocatalytic activity of the fibrous materials was investigated under UV irradiation using MB as a model organic pollutant. The degradation of MB was monitored spectrophotometrically at 662 nm by measuring the decrease in the absorbance as a function of irradiation time. The dependence of the photocatalytic degradation of MB on irradiation time for the different types of fibrous materials is shown in Figure 16. It can be seen that after 3 hours of irradiation, only 13% of MB (blank sample) is

degraded, while in the presence of PLDLLA fibers or Fe_3O_4-*in*-PLDLLA fibers, the degradation reaches 18% and 21%, respectively. These results indicate that UV irradiation leads to self-degradation of MB, but this process occurs at a very slow rate. The low degree of dye degradation in the presence of the materials of type "*in*" is likely due to its adsorption. It should be noted that the degradation of MB in the dark for 1 hour in the presence of the fibrous materials is similar to that of the blank sample (below 5%), which means that MB absorption onto the fibrous materials is limited after the adsorption–desorption equilibrium is reached (Figure 16). Under irradiation in the presence of the fibrous materials ZnO/QCOS-*on*-PLDLLA and ZnO/QCOS-*on*-(Fe_3O_4-*in*-PLDLLA), 50% of MB is degraded within 70 and 90 minutes, respectively. After 3 hours of irradiation, these materials degrade 88% and 92% of MB, respectively, indicating a nearly complete dye degradation in the presence of the materials of type "*on*" (Figure 16). This demonstrates that deposition of the photocatalyst ZnO onto the fiber's surface significantly enhances the photocatalytic activity and that ZnO retains its activity after the electrospraying.

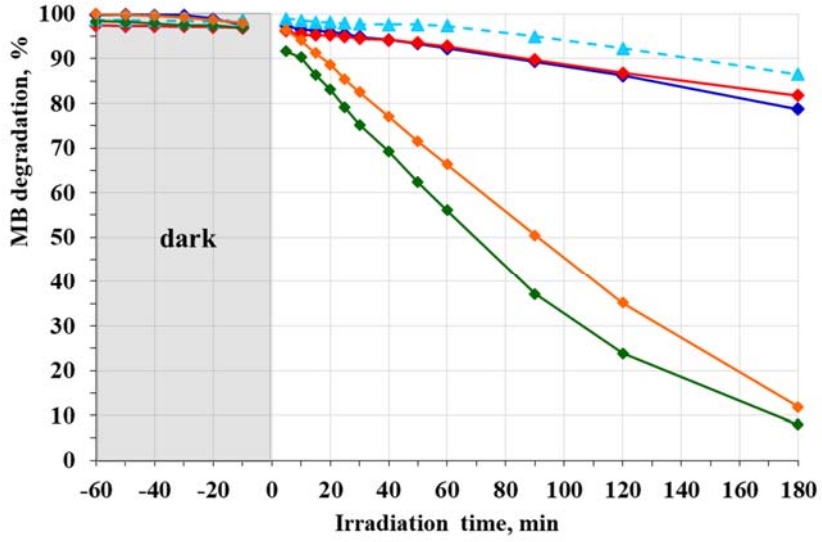

Figure 16. Photocatalytic degradation of MB at 662 nm in the presence of: PLDLLA (red line); Fe_3O_4-*in*-PLDLLA (dark blue line); ZnO/QCOS-*on*-PLDLLA (orange line); and ZnO/QCOS-*on*-(Fe_3O_4-*in*-PLDLLA) (green line). Blank sample – MB solution (light blue dashed line).

The reusability of the fibrous materials was also evaluated, as this is one of the key criteria for determining their applicability in large-scale water purification systems. The study was carried out by measuring the photocatalytic

activity of the fibrous materials over five consecutive irradiation cycles. The results show that the ZnO/QCOS-*on*-PLDLLA and ZnO/QCOS-*on*-(Fe_3O_4-*in*-PLDLLA) fibrous materials exhibit excellent reusability (Figure 17). After five irradiation cycles, these materials retain almost completely their photocatalytic activity, and at the end of the fifth cycle they degraded over 90% of MB. It should be noted that after the reusability test, the hybrid fibrous materials maintain high stability and show no visible structural changes: they preserve their shape and fibrous structure, and the weight loss is negligible, highlighting their mechanical and chemical durability.

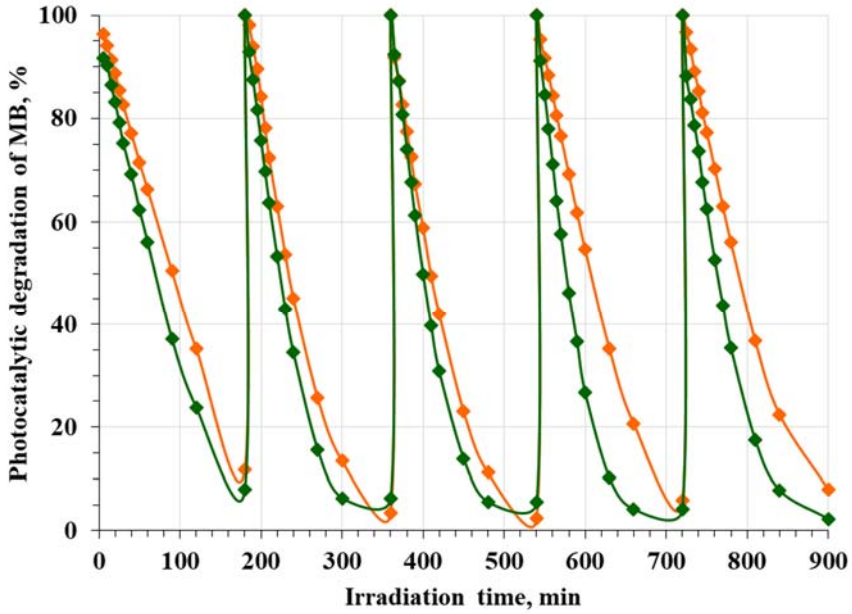

Figure 17. Photocatalytic degradation of MB over five consecutive irradiation cycles in the presence of: ZnO/QCOS-*on*-PLDLLA (orange line) and ZnO/QCOS-*on*-(Fe_3O_4-*in*-PLDLLA) (green line).

In conclusion, the results of **Chapter 2** demonstrate that a simple and effective one-step approach was proposed for the preparation of functional and environmentally friendly hybrid fibrous materials from PLDLLA. Fe_3O_4 particles were incorporated into the PLDLLA fibers to impart magnetic properties, while the deposition of ZnO particles onto the fiber's surface by electrospraying provided antioxidant and photocatalytic properties. It was shown that the inorganic particles influence the morphology, wettability, thermal properties, and crystallinity of the fibrous materials. The ZnO particles on the fiber's surface improve their wettability but slightly reduce the thermal stability of the materials of type "*on*". On the other hand, the incorporation of

Fe_3O_4 into the fibers and of ZnO onto the fiber's surface does not affect the amorphous structure of PLDLLA. The fibrous materials of type "*on*" with a purposely tailored design exhibit high antioxidant activity, with a DPPH• scavenging capacity of over 70% within 30 minutes. These materials exhibit high photocatalytic activity and stability, degrading the model organic pollutant methylene blue even after five consecutive irradiation cycles, reaching over 90% degradation by the end of the fifth cycle. Therefore, the obtained hybrid electrospun materials from PLDLLA, Fe_3O_4, and ZnO are promising candidates for the fabrication of environmentally friendly filters and water purification materials, enabling effective removal of organic pollutants and dyes by heterogeneous photocatalysis.

IV. CONCLUSIONS

Novel hybrid fibrous materials based on PLDLLA and chitosan derivatives with purposely tailored design have been obtained, and several possibilities for their potential applications have been demonstrated. Based on the conducted studies and the obtained results, the following main conclusions can be formulated:

1. For the first time, fibrous materials made of PLDLLA and the Schiff base of chitosan with 8-hydroxyquinoline-2-carboxaldehyde (Ch-8Q), as well as their complexes with the biologically significant Cu^{2+} and Fe^{3+} ions, have been obtained by electrospinning.

2. It has been demonstrated that the incorporation of Ch-8Q and the complex formation with Cu^{2+} and Fe^{3+} ions impart bactericidal activity to the fibrous materials, and that the fibrous materials of PLDLLA and Ch-8Q also exhibit a pronounced antiproliferative effect against human HeLa (cervical cancer) and MCF-7 (breast cancer) cells.

3. The new fibrous materials based on PLDLLA/Ch-8Q and their complexes with Cu^{2+} and Fe^{3+} are suitable candidates for biomedical applications as materials for wound treatment and as effective agents for local cancer therapy.

4. A set of hybrid fibrous materials based on PLDLLA, Fe_3O_4, and ZnO with purposely tailored design has been obtained by electrospinning or by combining electrospinning with electrospraying.

5. It has been demonstrated that the Fe_3O_4 incorporated into the PLDLLA fibers imparts to them magnetic properties, while the ZnO deposited on the surface of the PLDLLA fibers provides antioxidant and photocatalytic properties.

6. The new hybrid fibrous materials based on PLDLLA, Fe_3O_4, and ZnO may find potential application as materials for the purification of water from organic pollutants and dyes by heterogeneous photocatalysis.

V. CONTRIBUTIONS OF THE DISSERTATION AND DIRECTIONS FOR FUTURE RESEARCH

An important scientific contribution of the dissertation is that the Schiff base of chitosan with 8-hydroxyquinoline-2-carboxaldehyde has been synthesized for the first time, which opens new opportunities for the targeted functional modification of biopolymers.

A contribution with practical relevance is the developed original approach for obtaining a set of hybrid fibrous materials from PLDLLA and chitosan derivatives by combining electrospinning with various structural and functional engineering techniques - electrospinning followed by complexation with Cu^{2+} and Fe^{3+}, as well as its combination with electrospraying of ZnO.

Depending on their composition and design, the hybrid fibrous materials based on PLDLLA and chitosan derivatives have been shown to be promising candidates for applications in biomedicine and in the photocatalytic purification of water containing organic pollutants.

Based on the achieved results, **future research** will focus on the electrospinning of polymers from renewable sources and the incorporation of functional additives to impart photocatalytic and adsorption properties. The goal is to create new environmentally friendly materials for the purification of water from organic pollutants and heavy metals. In parallel, biocompatible and biodegradable fibrous materials will be developed by the inclusion of biologically active substances or nanoparticles with antimicrobial activity. In

this way, innovative fibrous systems will be developed to meet the needs of biomedicine and sustainable environmental protection.

VI. LIST OF PUBLICATIONS, CITATIONS AND SCIENTIFIC COMMUNICATIONS PRESENTING THE RESULTS OF THE DISSERTATION

PUBLICATIONS

[P 1] Ignatova, M., Anastasova, I., Manolova, N., Rashkov, I., Markova, N., Kukeva, R., Stoyanova, R., Georgieva, A., Toshkova, R. (**2022**). Bio-based electrospun fibers from chitosan Schiff base and polylactide and their Cu^{2+} and Fe^{3+} complexes: Preparation and antibacterial and anticancer activities. ***Polymers***, *14*, 5002; **Q1** (WoS), **IF$_{2022}$ 5,0.**

[P 2] Anastasova, I., Tsekova, P., Ignatova, M., Stoilova, O. (**2024**). Imparting photocatalytic and antioxidant properties to electrospun poly(L-lactide-*co*-D,L-lactide) materials. ***Polymers***, *16*, 1814; **Q1** (WoS), **IF$_{2024}$ 4,9.**

CITATIONS

[P 1] Ignatova, M., Anastasova, I., Manolova, N., Rashkov, I., Markova, N., Kukeva, R., Stoyanova, R., Georgieva, A., Toshkova, R. (**2022**). Bio-based electrospun fibers from chitosan Schiff base and polylactide and their Cu^{2+} and Fe^{3+} complexes: preparation and antibacterial and anticancer activities. ***Polymers***, *14*, 5002; **Q1** (WoS), **IF$_{2022}$ 5,0; *noted 13 citations:***

1. **Ragheb**, M.A., Salem, M.E., Hamed, A.A., Abdelhamid, I.A., Ali, H.A., Abdel-Megid, M., Elgamal, A.M. (**2025**). New isatin-chitosan Schiff base hybrids: Tri-functional bioactives for antimicrobial, anticancer, and antioxidant therapies supported by in silico docking and ADMET studies. *International Journal of Biological Macromolecules*, *331*, 148298.
2. **Zheng**, L., Zhu, Z., Pan, L., Zhong, L., Xiao, S., Zhao, C., Liu, Y., Xu, J., Zhang, Y. (**2025**). Polysaccharides and proteins as natural polymers for electrospun wound dressings: A review of healing potential, challenges, and crosslinking strategies. *International Journal of Biological Macromolecules*, *320*, 145960.
3. **Zou**, Q., Wu, Z., Cui, N., Zhang, Z., Wang, G. (**2025**). Research Progress in the Preparation and Application of Chitosan-Based Antimicrobial Fiber Materials. *Acta Chimica Sinica*, *83*(3), 287 – 298.
4. **Samokhin**, Y., Varava, Y., Diedkova, K., Yanko, I., Korniienko, V., Husak, Y., Iatsunskyi, I., Grebnevs, V., Bērtiņš, M., Banasiuk, R., Korniienko, V., Ramanaviciute, A., Pogorielov, M., Ramanavičius, A. (**2025**). Electrospun Chitosan/Polylactic Acid Nanofibers with Silver

Nanoparticles: Structure, Antibacterial, and Cytotoxic Properties. *ACS Applied Bio Materials*, *8*(2), 1027 – 1037.

5. **Chai**, Y., Luo, X., Lin, K., Zhang, H., Zhao, H., Cai, H., Hao, L. (**2025**). Anti-tumour and Angiogenic Properties of Cu^{2+} Coatings on Medical Mg-6Zn Alloy Prepared by Micro-arc oxidation. *Surface Technology*, *54*(4), 201 – 210.
6. **Gangadhar**, L., Sana, S. S., Mishra, V., Venkatesan, R., Kim, S.-C., Al-Tabakha, M. M. (**2025**). Recent Trends in Biomedical Applications of Cu_2MX_4-Based Nanocomposites: An Updated Review. *International Journal of Nanomedicine*, *20*, 11895 – 11939.
7. **Kanwal**, S., Bibi, S., Haleem, R., Waqar, K., Mir, S., Maalik, A., Sabahat, S., Hassan, S., Awwad, N.S., Ibrahium, H.A., Alturaifi, H.A. (**2024**). Functional potential of chitosan-metal nanostructures: Recent developments and applications. *International Journal of Biological Macromolecules*, *282*, 136715.
8. **Edo**, G.I., Yousif, E., Al-Mashhadani, M.H. (**2024**). Modified chitosan: Insight on biomedical and industrial applications. *International Journal of Biological Macromolecules*, *275*, 133526.
9. **Korniienko**, V., Husak, Y., Diedkova, K., Varava, Y., Grebnevs, V., Pogorielova, O., Bērtiņš, M., Korniienko, V., Zandersone, B., Ramanaviciene, A., Ramanavicius, A., Pogorielov, M. (**2024**). Antibacterial Potential and Biocompatibility of Chitosan/Polycaprolactone Nanofibrous Membranes Incorporated with Silver Nanoparticles. *Polymers*, *16*(12), 1729.
10. **Kuang**, G., Lin, X., Li, J., Sun, W., Zhang, Q., Zhao, Y. (**2024**). Electrospun nanofibers-derived functional scaffolds for cancer therapy. *Chemical Engineering Journal*, 489, 151253.
11. **Yang**, Y., Zhang, R., Liang, Z., Guo, J., Chen, B., Zhou, S., Yu, D. (**2024)**. Application of Electrospun Drug-Loaded Nanofibers in Cancer Therapy. *Polymers*, *16*(4), 504.
12. **Samokhin**, Y., Varava, Y., Diedkova, K., Yanko, I., Husak, Y., Radwan-Pragłowska, J., Pogorielova, O., Janus, Ł., Pogorielov, M., Korniienko, V. (**2023**). Fabrication and Characterization of Electrospun Chitosan/Polylactic Acid (CH/PLA) Nanofiber Scaffolds for Biomedical Application. *Journal of Functional Biomaterials*, *14*(8), 414.
13. **Iacopetta**, D., Ceramella, J., Catalano, A., Mariconda, A., Giuzio, F., Saturnino, C., Longo, P., Sinicropi, M.S. (**2023**). Metal Complexes with Schiff Bases as Antimicrobials and Catalysts. *Inorganics*, *11*(8), 320.

[P 2] Anastasova, I., Tsekova, P., Ignatova, M., Stoilova, O. (**2024**). Imparting photocatalytic and antioxidant properties to electrospun poly(L-lactide-*co*-D,L-lactide) materials. ***Polymers***, *16*, 1814; **Q1** (WoS), **IF_{2024} 4,9; *noted 1 citation*:**

1. **Palanisamy**, G., Bhosale, M., Magdum, S. S., Thangarasu, S., Oh, T. H. (**2024**). Hybridization of polymer-encapsulated MoS_2-ZnO nanostructures as organic–inorganic polymer films for sonocatalytic-induced dye degradation. *Polymers*, *16*(15), 2213.

SCIENTIFIC COMMUNICATIONS (*the name of the presenting author is underlined*):

Oral communications:

[OP 1] I. Anastasova, M. Ignatova, N. Manolova, I. Rashkov, N. Markova, A. Georgieva, R. Toshkova, Bio-based electrospun fibers from chitosan Schiff base and polylactide and their antibacterial and anticancer activities, 4th Interdisciplinary PhD Forum with International Participation, May 16 – 19 2023, Sandanski, Bulgaria.

[OP 2] I. Anastasova, M. Ignatova, N. Manolova, I. Rashkov, N. Markova, A. Georgieva, R. Toshkova, Fibrous materials from the Schiff base of chitosan and polylactide with antibacterial and anticancer activity, Third National Summer School on Natural Products with Applications in Medicine, June 27 – July 2, 2023, Burgas, Bulgaria.

[OP 3] I. Anastasova, M. Ignatova, N. Manolova, I. Rashkov, N. Markova, A. Georgieva, R. Toshkova, Innovative antibacterial and anticancer electrospun non-woven textile from chitosan Schiff base and polylactide and its complexes with Cu^{2+} and Fe^{3+}, XXV National Textile Conference with International Participation: Traditions and Innovations in Textiles and Clothing, October 26–28, 2023, Blagoevgrad, Bulgaria.

[OP 4] I. Anastassova, M. Ignatova, N. Manolova, I. Rashkov, N. Markova, A. Georgieva, R. Toshkova, Fibrous materials from the Schiff base of chitosan and polylactide with antibacterial and anticancer activity, presentation at the colloquium of the Institute of Polymers – BAS, November 10, 2023, Sofia, Bulgaria.

[OP 5] I. Anastasova, P. Tsekova, M. Ignatova, O. Stoilova, Electrospun hybrid materials based on poly(L-lactide-*co*-D,L-lactide) with antioxidant activity, 5th Interdisciplinary PhD Forum with International Participation, April 16 – 19, 2024, Kyustendil, Bulgaria.

[OP 6] I. Anastasova, P. Tsekova, M. Ignatova, O. Stoilova, Hybrid fibrous materials from poly(L-lactide-*co*-D,L-lactide) with antioxidant and photocatalytic activity, XVII Spring Seminar "Interdisciplinary Chemistry", April 23–25, 2024, Sofia, Bulgaria.

[OP 7] I. Anastasova, P. Tsekova, M. Ignatova, O. Stoilova, Design of hybrid fibrous materials from poly(L-lactide-*co*-D,L-lactide) for photocatalytic water

purification, Fifteenth Scientific Session "Young Scientists in the World of Polymers", June 6, 2024, Institute of Polymers – BAS, Sofia, Bulgaria.

[OP 8] I. Anastasova, P. Tsekova, M. Ignatova, O. Stoilova, Imparting photocatalytic and antioxidant properties to electrospun poly(L-lactide-*co*-D,L-lactide) materials, XXVI National Textile Conference with International Participation: Traditions and Innovations in Textiles and Clothing, October 17–19, 2024, Koprivshtitsa, Bulgaria.

[OP 9] I. Anastasova, P. Tsekova, M. Ignatova, O. Stoilova, Hybrid electrospun poly(L-lactide-*co*-D,L-lactide) materials with antioxidant and photocatalytic properties, International Seminar on Polymer Materials in Environmental and Climate Protection, July 17, 2025, Zabrze, Poland.

Poster communications:

[PP 1] I. Anastasova, M. Ignatova, I. Rashkov, N. Manolova, A. Georgieva, R. Toshkova, New electrospun materials from polylactic acid and a derivative of chitosan and 8-hydroxyquinoline: Preparation, characterization, and antitumor activity, Thirteenth Scientific Session "Young Scientists in the World of Polymers", June 2, 2022, Institute of Polymers – BAS, Sofia, Bulgaria.

[PP 2] I. Anastasova, M. Ignatova, I. Rashkov, N. Manolova, A. Georgieva, R. Toshkova, Novel antitumor electrospun materials from poly(lactic acid) and derivative of chitosan and 8-hydroxyquinoline, 20th National Symposium "Polymers 2022" with International Participation, July 5 – 8, 2022, Velingrad, Bulgaria.

[PP 3] I. Anastasova, M. Ignatova, N. Manolova, I. Rashkov, N. Markova, Hybrid fibrous materials from the Schiff base of chitosan and polylactide and their metal complexes with antibacterial activity, Fourteenth Scientific Session "Young Scientists in the World of Polymers", June 1, 2023, Institute of Polymers – BAS, Sofia, Bulgaria.

[PP 4] I. Anastasova, P. Tsekova, M. Ignatova, O. Stoilova, Design of electrospun hybrid materials based on poly(L-lactide-*co*-D,L-lactide) for antioxidant and photocatalytic performance, "NATO ASI Summer School for students from NATO countries and NATO Partner countries (Nanomaterials and Nanoarchitectures II. Composite Materials and their Applications)", June 28 – July 5, 2024, Smolenice, Slovakia.

[PP 5] I. Anastasova, P. Tsekova, M. Ignatova, O. Stoilova, Design of electrospun hybrid materials from poly(L-lactide-*co*-D,L-lactide) with antioxidant and photocatalytic activity, Sixteenth Scientific Session "Young Scientists in the World of Polymers", March 4, 2025, Institute of Polymers – BAS, Sofia, Bulgaria.

[PP 6] I. Anastasova, P. Tsekova, M. Ignatova, O. Stoilova, Hybrid electrospun poly(L-*co*-D,L-lactide) materials with antioxidant and photocatalytic

properties, 21st National Symposium “POLYMERS 2025” with International Participation, June 29 – July 2, 2025, Kazanluk, Bulgaria.

AWARDS

For an excellent oral presentation at the 4th Interdisciplinary PhD Forum with International Participation, Sandanski, May 2023

For the best poster presentation at the Fourteenth Scientific Session “Young Scientists in the World of Polymers”, organized by the Institute of Polymers – BAS, Sofia, June 2023

Special award at the Third National Summer School on Natural Products with Applications in Medicine, Burgas, June 2023

“Prof. Ivan Shopov” Award for Outstanding Young Scientist in the Field of Polymers, March 2025

PARTICIPATION IN SCIENTIFIC PROJECTS

Center of Competence: **BG05M2OP001-1.002-0012-C01**, Sustainable Utilization of Bio-Resources and Waste from Medicinal and Aromatic Plants for Innovative Bioactive Products, funded by the Operational Programme “Science and Education for Smart Growth”, co-financed by the European Union by the European Structural and Investment Funds.

National Center of Excellence Mechatronics and Clean Technologies: **BG16RFPR002-1.014-0006**, funded by the Program “Research, Innovation and Digitalization for Smart Transformation” 2021–2027, co-financed by the European Union by the European Regional Development Fund.